Gating, Modulation, and Targeting of NMDA Receptors

by

Christopher G. Thomas

A Dissertation

Presented to The Neuroscience Graduate Program

and to The Oregon Health and Science University School of Medicine

in partial fulfillment of the requirements of

Doctor of Philosophy

June 2005

School of Medicine

Oregon Health and Science University

CERTIFICATE OF APPROVAL

This is to certify that the Ph.D. thesis of Christopher G. Thomas has been approved.

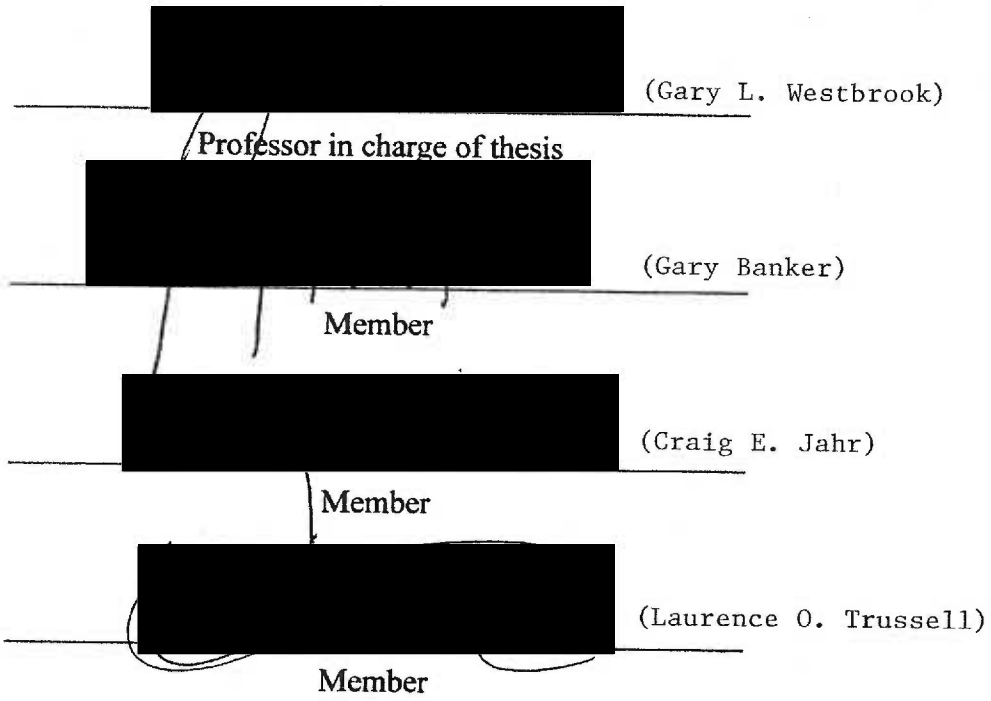

Table of Contents

Acknowledgements

I thank my mentor Gary Westbrook for his support, inspiration, and, most importantly, for showing me how to use a reductive approach to science. My time in Gary's lab significantly changed the way I think and work for the better and I'm thoroughly indebted to Gary for his guidance.

I thank Johannes Krupp, a former post-doc in the lab, who showed me how to do electrophysiology and provided significant guidance to this thesis. He was a second mentor and I'm equally indebted to him as I am to Gary.

I thank Ken Tovar for being a friend both in and outside of the lab. He also provided guidance to this thesis.

I thank research assistants, Ashleigh Miller, Lindsay Grimes, Forrest Davis and Robert Mouton for their help with molecular biology and cell cultures.

I thank Stephani and Jamie Sutherland for welcoming me into their home for four years, for being good friends throughout the years, and for introducing me to snowboarding.

Finally, I thank my parents for their love and support and for tolerating my nine years away.

Abstract

N-Methyl-D-Aspartic Acid (NMDA) receptors, found at most glutamatergic synapses throughout the central nervous system, mediate the slow component of excitatory postsynaptic responses (Figure 1; McBain and Mayer 1994). NMDA receptor channel kinetics are especially important for defining postsynaptic responses because NMDA receptors are active long after glutamate has been cleared from the synaptic cleft (Clements et al. 1992; Lester et al. 1990). The structure of an ion channel underlies its gating movements and its interactions with other proteins. Therefore the structure of the NMDA receptor ultimately contributes to the sizes and shapes of postsynaptic responses. My thesis work examined the modulation of NMDA receptor activity by intracellular proteins, the relationship between subunit composition and receptor targeting, and conformational changes associated with receptor gating. The introduction reviews NMDA receptor structure and function with a focus on the three aforementioned topics whereas the subsequent chapters describe the studies on receptor targeting and receptor gating.

Introduction

NMDA Receptor Subunits

NMDA receptors were defined by their functional properties as ionotropic glutamate receptors that are selectively opened by NMDA (in the presence of glycine), are selectively blocked by AP5, are blocked by magnesium in a voltage-dependent manner, and have high calcium permeability (McBain and Mayer 1994). NMDA receptor activity is involved with synaptic plasticity, neuronal development, and diseases. Cloning of the glycine-binding NR1 and glutamate-binding NR2 subunits revealed that NMDA receptors are, indeed, a subtype of the ionotropic glutamate receptor family, characterized by a secondary structure (Figure 2) that has a large extracellular, N-terminal domain, four transmembrane domains (M1-4), and an intracellular C-terminal domain (Figure 2; Wollmuth and Sobolevsky 2004). M2 is a reentrant loop that defines the channel pore. A large extracellular domain connects M3 and M4. NMDA receptors are thought to be tetramers of two NR1s and two NR2s, arranged in an NR1-NR1-NR2-NR2 order (Schorge and Colquhoun 2003). A glycine-binding NR3 subunit can reduce NMDA receptor activity when coexpressed with NR1 and NR2 subunits or can form a glycine-activated receptor with NR1 subunits (Chatterton et al. 2002). However NR3 subunits are expressed in only a few cells in the central nervous system and are not present in hippocampal pyramidal neurons. Thus in this thesis I will discuss NMDA receptors that are multimers of NR1 and NR2 subunits.

There is one NR1 gene but eight splice variants (Hollmann et al. 1993). These variants are determined by the presence of inserts in the extracellular N- and intracellular C-terminal domains as well as a second intracellular C-terminal cassette

(Figure 2). NR1 subunits are ubiquitously expressed throughout the central nervous system with the NR1-1a subunit being the most abundantly expressed variant (McBain and Mayer 1994). In contrast, there are four NR2 genes (NR2A-NR2D) that have different expression patterns (Monyer et al. 1994). NR2B is expressed throughout the entire embryonic rodent brain whereas NR2D subunits are only present in the diencephalon and brain stem. During the first two postnatal weeks NR2A expression appears throughout the rest of the rodent brain whereas NR2C is expressed primarily in the cerebellum. It has been reported that NR2C is also expressed in the hippocampus between 7 and 14 postnatal days (Pollard et al. 1993). However hippocampal neurons from transgenic mice that lack NR2A and NR2B subunits do not have NMDA receptor currents (unpublished data). This is an important point because the first manuscript of this thesis assumes that hippocampal neurons express only NR1, NR2A, and NR2B subunits.

NR2 subunits determine many of the differences in activity between NMDA receptors subunit combinations. The affinities of recombinant NR1/NR2 receptors for glutamate and glycine increase in the following order: NR2A, NR2B, NRC, and NR2D (Kutsuwada et al. 1992). Single channel currents of receptors containing NR2A or NR2B have higher conductances (Edmonds et al. 1995), are blocked by lower concentrations of magnesium, and have greater open probabilities than receptors containing NR2C or NR2D subunits (McBain and Mayer 1994). Receptors containing NR2A and NR2B subunits also show glycine-independent desensitization whereas receptors containing NR2C and NR2D do not (Krupp et al. 1996; Monyer et al. 1994). NR1/NR2A-containing receptors have a greater peak open probability (Chen et al.

1999; Erreger et al. 2005), display more macroscopic desensitization, and recover from desensitization more quickly than NR1/NR2B-containing receptors (Vicini et al. 1998). These differences have direct effects on synaptic responses. For instance, the deactivation of NMDA receptor mediated EPSCs with NR1/NR2A-containing receptors are significantly faster than those with NR1/NR2B-containing receptors (Tovar et al. 2000).

The Channel

All NMDA receptor subunits have the same secondary structure that can be divided both structurally and functionally into three parts: extracellular domains, transmembrane domains, and intracellular C-terminal domains (Figure 3). Transmembrane domains are the most homologous parts of NMDA receptor subunits and they are functionally associated with the channel. There are four transmembrane domains, M1-M4. The NMDA receptor channel is thought to look like an inverted potassium channel, with a narrow pore and a large extracellular vestibule (Wollmuth and Sobolevsky 2004). M2 is a reentrant loop, reminiscent of the potassium channel P-loop. A conserved M2 asparagine residue, that controls calcium and magnesium permeability, in NR1 and NR2 subunits aligns well with the pore-forming threonine of potassium channels that is located at the tip of the P-loop (Kuner et al. 2003). Experiments using the substituted-cysteine accessibility method (SCAM) support the idea that these asparagines in M2 form the NMDA receptor selectivity filter (Kuner et al. 1996). Further experiments using SCAM suggested that M3 lines the extracellular vestibule with parts of M1 and M4 contributing to the outer portion of the vestibule

(Beck et al. 1999). The M3 domain of all NMDA receptor subunits contain a motif (SYTANLAAF) that is conserved throughout all ionotropic glutamate receptors. The lurcher mutation, which substitutes the third alanine residue with a threonine (SYTANLAAF>SYTANLATF), dramatically affects the gating of ionotropic glutamate receptors. This mutation causes some AMPA receptors to open in the absence of agonist, it eliminates the fast component of NMDA receptor desensitization when introduced into either subunit, and it greatly lengthens deactivation when introduced into NR1 subunits (Kohda et al. 2000). The conservation of the SYTANLAAF motif combined with the fact that mutations in it affect gating suggest that it may be the activation "gate" that couples ligand binding to channel gating in all ionotropic glutamate receptors (Wollmuth and Sobolevsky 2004).

Extracellular Domains

Ligand-binding domains

Extracellular domains are the second most homologous parts of NMDA receptor subunits and they are involved in agonist binding, surface expression of functional receptors, and receptor modulation. These domains include the large N-terminal domain and the loop connecting M3 with M4. The extracellular domains of all ionotropic subunits contain two regions that are homologous to bacterial periplasmic binding proteins (Mayer and Armstrong 2004). One of these regions, resembling the lysine/arginine/ornithine-binding protein (LOABP), is divided between a portion of the N-terminus, called S1, and a portion of the loop connecting M3 with M4, called S2. Crystal structures from the S1 and S2 domains of AMPA and KA receptors show that

LOABP-like domains dimerize through noncovalent S1-S1 interactions and that S1 and S2 domains form a clamshell around the ligand (Sun et al. 2002). Closing of S2 regions around the ligand may move M3 domains enough to cause gating. The structure of the homologous NR1 domain did not dimerize but the S1 and S2 domains did close around glycine (Furukawa and Gouaux 2003). Site-directed mutagenesis studies on NR2 subunits suggest that their S1 and S2 domains also form a clamshell around glutamate (Chen et al. 2005; Laube et al. 2004). These similarities between AMPA and NMDA receptor ligand-binding cores suggest that NMDA receptor gating begins with S2 region closure, resulting in M3 domain movement and channel opening.

LIVBP-like domains

The first 400, N-terminal amino acids of the NMDA receptor extracellular region are highly homologous to the bacterial periplasmic binding protein, leucine/isoleucine/valine binding-protein (LIVBP; Herin 2004). LIVBP-like domains of NR2 subunits bind zinc resulting in modulation of channel activity (Paoletti et al. 2000). At low concentrations, zinc inhibits NMDA currents and increases desensitization in a voltage-independent manner whereas at high concentrations zinc block is voltage-dependent (Herin 2004). NR1a/NR2A receptors are much more sensitive to zinc modulation than NR1a/NR2B or NR1a/NR2C receptors (Paoletti et al. 1997). With an approximate IC_{50} of 10 nM, the amount of zinc in extracellular solutions can partially block NR1a/NR2A receptors (Zheng et al. 2001). Structural studies suggest that the LIVBP-like domain of NR2A also has two lobes that close like a clamshell around a molecule of zinc, similar to S1/S2 domain closure around glutamate or glycine (Paoletti

et al. 2000). Voltage-independent zinc block is use-dependent such that the binding of glutamate increases zinc affinity and vice versa (Zheng et al. 2001). In addition, zinc block increases proton inhibition of NR1/NR2A receptors. Recent studies have shown that residues in M3 and around the lurcher motif of NR1 and NR2A are responsible for proton inhibition (Low et al. 2003). Thus, it is thought that following zinc binding to the LIVBP-like domain of NR2A subsequent conformational changes occur in the S1/S2 domain and lurcher motifs of NR1 and NR2A resulting in increased channel closure.

Ifenprodil, the NR2B-selective antagonist used in Chapter 1, binds with high affinity to the LIVBP-like domain of NR2B causing the two lobes to close (Perin-Dureau et al. 2002). Inhibition by ifenprodil is use-dependent and increases proton inhibition of NMDA receptors (Mott et al. 1998). Thus it is thought that the mechanism of ifenprodil inhibition of NR1/NR2B receptors is similar to that caused by voltage-independent zinc inhibition of NR1/NR2A receptors.

The LIVBP-like domains of NR1 also influence voltage-independent zinc block and ifenprodil inhibition. The LIVBP-like domains of NR1b contain a 21 amino acid insert that renders NR1b/NR2A and NR1b/NR2B receptors less sensitive to voltage-independent zinc block (Paoletti et al. 1997). The mechanism for this reduction is not known. Nevertheless the NR1b insert reduces proton inhibition (Traynelis et al. 1995), suggesting that it reduces voltage-independent zinc block by affecting the confirmation of the proton-sensing residues in and around the lurcher motif. Mutations in the NR1 LIVBP-like domain have been shown to reduce the ifenprodil inhibition of NR1/NR2B receptors (Masuko et al. 1999). Currently it is not known whether those mutations inhibited the two lobes of NR1 LIVBP-like domains from closing or whether the

mutations indirectly destabilized ifenprodil/NMDA receptor complexes (Perin-Dureau et al. 2002).

The LIVBP-like domain of NR1 not only modulates receptor activity, it is also necessary for NMDA receptor assembly. *In vitro* experiments have shown that surface expression of NR2A requires NR1 subunits whereas surface expression, but not functional expression, of most NR1 subunit variants does not require NR2 (Okabe et al. 1999). The NR1 LIVBP-like domain is also required for cell surface expression of NR1/NR2A multimers and oligomerization of NR1 homodimers (Meddows et al. 2001). The absence of NR1 LIVBP-like domains may explain why NR1 agonist binding core crystals did not dimerize in the experiments mentioned above. Whether NR1 LIVBP-like domains directly mediate intersubunit interactions or merely stabilize them is not known yet. Nevertheless these results suggest that functional expression of NMDA receptors requires direct interactions between the N-terminal domains of NR1 and NR2 subunits, similar to those seen with AMPA and KA receptors.

Glycine-dependent desensitization

Heteromeric interactions between the N-terminal domains of NR1 and NR2 subunits are responsible for glycine-dependent desensitization. Glycine-dependent desensitization occurs when NMDA receptors are activated with high amounts of glutamate in the presence of low glycine (1 μM). Glutamate binding decreases glycine affinity resulting in a current that peaks and then decreases to a steady state during the glutamate application (Mayer et al. 1989; McBain and Mayer 1994). NR1/NR2A receptors have a lower affinity for glycine and are thus more affected by glycine-

dependent desensitization than NR1/NR2C receptors. Using recombinant chimerc mutants of NR2A and NR2C subunits Regalado et al. (2001) showed that S1 residues near the LIVBP-like domain of NR2 are responsible for the differences in glycine affinity. Conversely, mutations in homologous NR1 residues influence glutamate affinity. Thus the S1 domains influence the heteromeric cooperativity responsible for glycine-dependent desensitization.

Glycine-independent desensitization

N-terminal domains of NR2 subunits are also responsible for glycine-independent desensitization (Krupp et al. 1998; Villarroel et al. 1998). This form of desensitization reflects a state in which the channel is closed even though the receptor remains fully bound by agonists (Colquhoun and Hawkes 1995). It had been proposed that desensitization represented the closing of a part of the channel that was different than the activation gate; i.e. a desensitization gate (Sobolevsky et al. 1999). Such desensitization occurs in receptors containing NR2A or NR2B subunits but not NR2C. Studies using recombinant NR2A/NR2C chimeras showed that the LIVBP-like domain and the pre-M1 region of NR2A control glycine-independent desensitization (Krupp et al. 1998; Villarroel et al. 1998). Further studies showed that voltage-independent zinc inhibition, mediated by the LIVBP-like domain, controls the fast component of macroscopic desensitization, leaving the slow component to be mediated by the pre-M1 region (Zheng et al. 2001). SCAM studies showed that the pre-M1/M1 region of NR1 contributes to the extracellular vestibule (Beck et al. 1999). For these reasons and because it links the S1, agonist binding domain with the M1 domain, the pre-M1 region

may couple ligand binding with channel gating. Therefore, in Chapter 2, we used SCAM to study conformational changes in the pre-M1 region and M1 domain associated with desensitization.

Intracellular C-terminal Domains

The intracellular, C-terminal domains provide the most diversity among NMDA receptor subunits. NR2 intracellular domains are much longer than NR1 subunits and the intracellular sequences of all NMDA receptor subunits, including NR1 variants, differ from each other. In general, the intracellular C-terminal domains mediate interactions with intracellular proteins (Wenthold et al. 2003). The diversity of interactions subunits make reflects their sequence differences. NR1 subunits can interact with alpha-actinin, calcium/calmodulin, membrane-associated guanylate kinases (MAGUKs), myosin II regulatory light chain (MRLC) (Amparan et al. 2005), neurofilament subunit L (NF-L), protein kinase A, protein kinase C, receptor tyrosine kinases, spectrin, tubulin, and yotiao (Wenthold et al. 2003). Interactions with these proteins can depend on the C-terminal cassettes of the NR1 splice variants. Although there are some differences, NR2A and NR2B subunits can interact with: alpha-actinin, adaptor protein 2 (AP2) subunits μ1, μ2, and μ4, calcium/calmodulin kinase II, phospholipase C-γ, spectrin, tubulin, the non-receptor tyrosine kinase, src, and MAGUKs, like PSD-95, PSD-93, and SAP102, and other PDZ binding proteins, specifically S-SCAM, CIPP, m-Lin-7. These interactions can influence NMDA receptor activity, trafficking, and targeting (Wenthold et al. 2003).

NR1 interactions with Ca^{2+}/calmodulin and α-actinin modulate Ca^{2+}-dependent inactivation

The C0 domain is present in the C-termini of all NR1 subunits, and because of its presence all NR1 subunits can bind to alpha-actinin (α-actinin) and calcium/calmodulin (Ca2+/calmodulin; Ehlers et al. 1996; Wyszynski et al. 1997). These interactions are important because, as our lab and others have demonstrated, they influence calcium-dependent inactivation of NMDA receptors (Krupp et al. 1999; Zhang et al. 1998). Calcium-dependent inactivation is a reduction in NMDA receptor open probability (P_o) resulting from increased intracellular calcium (Legendre et al. 1993). Calcium influx through NMDA receptors is sufficient to induce inactivation. Previous results showed that α-actinin can compete with Ca^{2+}/calmodulin for C0 or the alternatively-spliced, intracellular cassette, C1 (Wyszynski et al. 1997). Whole-cell recordings of recombinant NR1/NR2A receptor currents from our lab showed that amino acids 858 to 863 of C0 domains are required for inactivation (Krupp et al. 1999). Overexpression of calcium-insensitive α-actinins greatly reduced or eliminated inactivation that was recovered by adding Ca^{2+}/calmodulin in the electrode. Using the IAsys binding assay system we confirmed that α-actinin can bind to a peptide containing the C0 amino acid sequence with lower affinity than Ca^{2+}/calmodulin. C0 peptides engineered to mimic truncation and point mutations that eliminated or reduced inactivation, decreased Ca^{2+}/calmodulin affinity. Interestingly, the open probability of NR1 truncation mutants lacking parts of the C0 domain was lower than normal,

suggesting that C0 itself affects P_o. From these results, we concluded that there are calmodulin-independent and calmodulin-dependent inactivation mechanisms. In calmodulin-independent inactivation, calcium-sensitive α-actinin, bound to C0, "hold" the receptors at a certain P_o. Elevated calcium causes α-actinin to unbind from C0, which, by itself, may induce a reduction of P_o. In calmodulin-dependent inactivation elevated calcium causes Ca^{2+}/calmodulin to compete α-actinin off of C0 decreasing P_o. I contributed to this project by performing the IAsys binding assays.

Calcineurin modulates desensitization through the intracellular domain of NR2A

Elevated intracellular calcium can activate phosphatase IIb, or calcineurin, leading to a reduction in the amplitude of NMDA receptor currents and an increase in glycine-independent desensitization (Tong and Jahr 1994). I also contributed to a study in which our lab used whole-cell recordings of recombinant NR1/NR2A currents to demonstrate that the intracellular domain of NR2A was involved with calcineurin modulation (Krupp et al. 2002). Truncation of NR2A at residue 905 eliminated calcineurin modulation, resulting in currents that were stable throughout our recordings, whereas truncation at residue 854 permanently enhanced desensitization without affecting the peak amplitude. Serine-to-alanine point mutations, made in full-length NR2A subunits at potential phosphorylation sites between residues 838 and 932, revealed that mutation of the 929 residue eliminated calcineurin modulation. By contrast, mutation of residue 900 enhanced desensitized without affecting the peak amplitude. These results suggested that residue 900 is the residue that calcineurin dephosphorylates and that dephosphorylation of the 929 residue blocks interactions with

calcineurin by possibly inducing a "protective" confirmation of the NR2A intracellular domain or by binding another intracellular protein that blocks calcineurin access.

Targeting, trafficking and intracellular domains

The first chapter of this thesis examines whether there are differences in the targeting of NR2A and NR2B subunits between synaptic and extrasynaptic NMDA receptors in developing hippocampal cultures and whether truncation of the NR2A intracellular domain affects targeting. We examined these issues because it is currently unclear whether there are targeting differences between NR2A and NR2B subunits. This controversy is interesting because it is thought that targeting and trafficking are mediated by interactions between intracellular proteins and the C-termini of NMDA receptor subunits (Nong et al. 2004; Perez-Otano and Ehlers 2004; Wenthold et al. 2003). Recordings from neurons expressing either C-terminally truncated NR2A or NR2B subunits showed a reduction in synaptic NMDA receptors (Mohrmann et al. 2002; Steigerwald et al. 2000). These results suggest that truncation disrupted the targeting and trafficking of NMDA receptors. Whether truncation disrupted receptor assembly, delivery of receptors to the plasma membrane, receptor clustering at synapses, or the internalization of receptors was not determined.

Receptor assembly

When expressed alone in heterologous cells, NR1-1 and NR2 subunits accumulate in the ER (McIlhinney et al. 1998). Other NR1 subunits can reach the plasma membrane but do not form functional receptors (Okabe et al. 1999). Thus the

ER is thought to be the site where functional NMDA receptors are assembled. The intracellular C1 and C2' cassettes of NR1 subunits have been implicated in ER trafficking (Standley et al. 2000). The C1 cassette, present in NR1-1 and NR1-3, has the ER retention motif RXR (RRR) whereas the divaline residues on the end of the C2' cassette, present in NR1-3 and NR1-4, are a coat protein complex II (COPII) binding motif (Barlowe 2003). Mu et al. (2003) suggest that NR1-3 subunits do not accumulate in the ER because C2'/COPII interactions relieve ER retention. Phosphorylation of serines flanking the RXR motif by PKC or PKA relieves NR1-1 retention, possibly by masking the RXR motif (Scott et al. 2003). Coassembly with NR2 subunits also relieves ER retention of NR1-1 subunits (McIlhinney et al. 1998). Coexpression of NR1-1a subunits with the C-terminal truncation mutant of NR2A ($NR2A_{stop844}$) in HEK293 cells results in functional NMDA receptors. $NR2A_{stop844}$ contains only the first seven amino acids of the intracellular domain and therefore almost no binding motifs. Thus coassembly may relieve NR1-1 retention by means other than masking the RXR motif.

Exocytosis

It is thought that newly processed NMDA receptors are transported from the Golgi to the plasma membrane as vesicles via exocytosis. Vesicular transport of NMDA receptors was indirectly demonstrated in oocytes when Lan et al. (2001) showed that PKA increased NMDA receptor surface expression in a SNARE-dependent manner. Two studies suggest that the intracellular domains of NR2 may be involved with exocytosis. Sans et al. (Sans et al. 2003; 2003) showed that in rat brain extracts the NR2B subunit forms a complex with the anchoring protein, SAP102 and the sec8

exocyst protein. The exocyst is a protein complex involved in transporting vesicles from the Golgi to the plasma membrane (Hsu et al. 1999) and Sans et al. (2003) suggested that SAP102 links NR2B subunits to exocyst complexes. The intracellular domain of NR2B and the sec8 protein have PDZ binding motifs that SAP102 recognizes. Elimination of the sec8 PDZ binding motif reduced NR2B surface expression in transfected neurons, suggesting that the exocyst contributes to trafficking.

The NR2B subunit can also be linked to KIF17, a kinesin superfamily motor protein, through the mLin-10, mLin-7, and mLin-2 scaffolding protein complex. mLin proteins are anchoring proteins that also contain PDZ binding domains (Setou et al. 2000). NR2B/KIF17 clusters do not colocalize with synaptic markers suggesting extrasynaptic targeting (Guillaud et al. 2003). Knockdown of KIF17 expression with antisense KIF17 cDNA reduced NR2B expression and increased NR2A expression. Conversely, treatment with AP5 increased KIF17 and NR2B expression. Thus these results suggest that there may be exocytic "pathways" that are subunit specific if not also specific for synaptic and extrasynaptic sites.

Receptor trapping and clustering

NMDA receptors can move laterally in the plasma membrane between synaptic and extrasynaptic sites (Tovar and Westbrook 2002). It is hypothesized that extrasynaptic NMDA receptors provide a pool of reserve receptors, ready to enter the synapse, and that NMDA receptors are clustered at synapses by intracellular interactions with postsynaptic density (PSD) proteins (Perez-Otano and Ehlers 2004).

Activation of PKC increases the lateral mobility of NMDA receptors supporting the idea that intracellular proteins modulate lateral mobility (Groc et al. 2004).

The MAGUK anchoring proteins are likely candidates for NMDA receptor clustering proteins because they are highly clustered at PSDs, they are consistently members of NMDA receptor complexes (Kim and Sheng 2004), they cause clustering of NMDA receptor subunits when coexpressed in heterologous cells (Kim et al. 1996), and they can inhibit NMDA receptor internalization (Lavezzari et al. 2003; Lin et al. 2004). These postsynaptic proteins include PSD-95, SAP102, and PSD-93. All three of these proteins have three PDZ binding domains, a src homology domain 3 (SH3), and a catalytically inactive guanylate kinase domain that is another anchoring site (Kim and Sheng 2004). The last four amino acids of NR2 subunits and of the C2' cassette of NR1 subunits are PDZ binding motifs. Elimination of the PDZ binding domains of NR2A and NR2B subunits reduced their incorporation into synapses (Barria and Malinow 2002). However it is not clear whether these results reflect decreased clustering or disruption of trafficking. Sans et al. (2000) showed that NR2A and PSD-95 expression coincide, they are highly associated with each other in rat brain extracts, and that NR2A binds better to PSD-95 than to SAP102. NR2B shows a similar link to SAP102. Immunogold electron microscopy shows that PSD-95 colocalizes with NR2A subunits at synapses whereas SAP102 colocalizes with NR2B subunits at extrasynaptic sites. These results suggest that MAGUKs are members of NMDA receptor complexes and that their interactions with other intracellular proteins might help define whether receptors are synaptic or extrasynaptic.

Endocytosis

Internalization of receptors may also influence NMDA receptor distribution. Biochemical studies have shown that NMDA receptor internalization decreases as young neurons mature and the fraction of synaptic NMDA receptors increases (Roche et al. 2001). Whole-cell recordings from cultured hippocampal neurons have indicated that extrasynaptic NMDA receptors are more susceptible to use-dependent decline in peak current than synaptic receptors (Li et al. 2002). Because use-dependent decline of peak current is caused by a decrease in the number of receptors, presumably due to clathrin-mediated endocytosis (Vissel et al. 2001), these results suggest that extrasynaptic NMDA receptors are more susceptible to internalization than synaptic receptors. Clathrin-coated vesicles in young neurons rapidly assemble and disassemble throughout dendrites (Blanpied et al. 2002). In contrast, endocytosis in older neurons occurs at sites outside of the PSD (Racz et al. 2004). Overall these results support the notion that internalization occurs at extrasynaptic sites whereas synaptic sites are more stable.

Endocytic binding motifs are located on the intracellular, C-terminal domains of NR1 and NR2 subunits. Tyrosine residues on the C-termini of NR1 and NR2 subunits that are located proximally to the end of M4 are part of a binding motif (YXXΦ, Φ represents a large hydrophobic residue) for the μ2 subunit of the adaptor protein AP-2 (Vissel et al. 2001). Activation of the tyrosine kinase src blocks use-dependent decreases in NMDA receptor currents presumably by phosphorylating these tyrosines and blocking μ2 binding. Scott et al. (2004) suggested that internalization mediated by the proximal tyrosines targets receptors to late endosomes and thus protein degradation. C-terminal truncation mutants of NR1 or NR2 subunits require the proximal tyrosines

for functional expression (unpublished data), suggesting these residues may also be involved in NMDA receptor assembly and exocytosis.

The distal portions of the C-termini of NR2A (residues 1304 - 1464) and NR2B (1315 - 1482) subunits each have dileucine and YXXΦ endocytic motifs (Nong et al. 2004; Wenthold et al. 2003). Internalization of the NR2B C-terminus appears to be dependent on the YXXΦ motif whereas internalization of the NR2A C-terminus is dependent on the dileucine motif (Lavezzari et al. 2004). A yeast-two hybrid assay showed that the distal portions of both NR2A and NR2B interacted equally well with the μ1 subunit of AP-2 but that NR2B interacted more strongly than NR2A with the μ2 subunit. Lavezzari et al. (2004) showed that the NR2B C-terminus undergoes constitutive endocytosis faster than the NR2A C-terminus. The NR2B C-terminus was also targeted to recycling vesicles whereas the NR2A C-terminus was targeted to lysosomal vesicles. If these results apply to intact NMDA receptor complexes then they support the idea that differences in NMDA receptor internalization may also contribute to differential targeting of NR2 subunits.

The background information provided in this introduction supports the studies described in the next chapters. Chapter 1 uses whole-cell recording techniques to examine the distribution of NR2A and NRB subunits during synaptic development and whether the intracellular C-terminal domain of NR2A influences its distribution. Chapter 2 uses the substituted-cysteine scanning mutagenesis method to determine whether the accessibility of residues in the pre-M1 region and M1 domain of NR1/NR2A receptors changes during glycine-independent desensitization.

Figure Legends

Figure 1. NMDA receptors mediate the second component of excitatory responses at fast glutamatergic synapses. A, left panel: Diagram of a glutamatergic synapse. The presynpatic bouton contains glutamate-filled vesicles. The postsynaptic cell expresses two types of ionotropic glutamate receptors, AMPA receptors and NMDA receptors. These receptors are closely apposed to the presynaptic bouton and are part of a dense protein network called the postsynaptic density. A, right panel: When an action potential invades a presynaptic bouton it can cause release of glutamate. The glutamate travels across the synaptic cleft where it can bind to AMPA and NMDA receptors. Glutamate-binding can activate the postsynaptic receptors resulting in the opening of their ion channels and, ultimately, ion conduction. B: Examples of excitatory postsynaptic currents (EPSCs) recorded from an autaptic hippocampal neuron (Tovar et al. 2000). Recordings were made in whole-cell voltage-clamp mode. Tovar et al. (2000) induced transmitter release by depolarizing the cell to +10 mV for 500 μsec. EPSCs recorded in control solution have fast and slow components. The AMPA receptor antagonist, NBQX, eliminated the fast, AMPA receptor-mediated component of EPSCs whereas the NMDA receptor antagonist, AP5, eliminated the slow, NMDA receptor-mediated component.

Figure 2. NMDA receptors are heteromers of NR1 and NR2 subunits. A: Diagrams of the secondary structures of NR1 and NR2 subunits. Both subunits contain two large extracellular domains, four transmembrane domains, and an intracellular C-terminal domain. NR1 subunits have shorter C-termini than NR2s. There is one NR1 gene and

four NR2 genes (NR2A-NR2D). Post-translational modification of NR1 subunits results in eight variants. NR1 variants are determined by the presence of extracellular and intracellular (C1) inserts and on whether the subunit contains a C2 or C2' cassette at the end of the intracellular C-terminal domain. B: NMDA receptors are thought to be tetramers of NR1 and NR2 subunits arranged in an NR1-NR1-NR2-NR2 order as shown here. NR1 subunits bind to glycine whereas NR2 subunits bind to glutamate. Two molecules of glycine and two molecules of glutamate are required for receptor activation (Clements and Westbrook 1991).

Figure 3. The NMDA receptor subunit structure is functionally modular. Extracellular domains are responsible for ligand binding, modulation by extracellular factors, like zinc, and assembly of functional receptors. Transmembrane domains form the channel and are involved in channel block by magnesium and calcium permeability. C-terminal domains interact directly with intracellular proteins. These interactions modulate NMDA receptor activity, regulate receptor assembly and trafficking, and form signaling complexes.

Figure 1

A

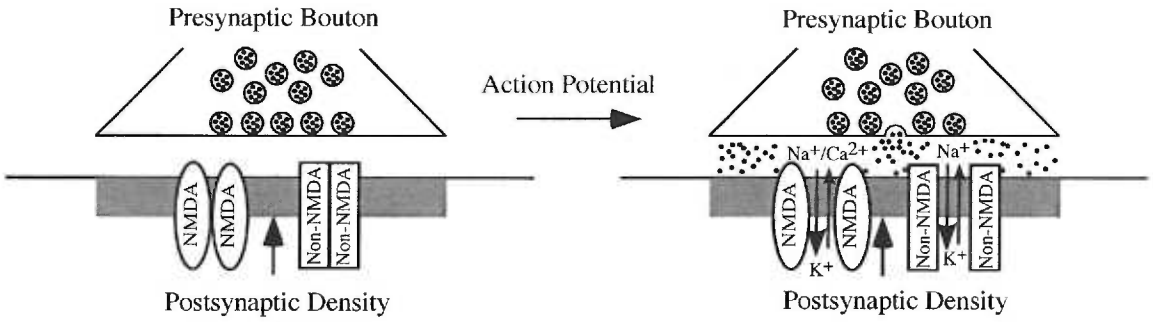
Presynaptic Bouton
Action Potential
Presynaptic Bouton
NMDA
NMDA
Non-NMDA
Non-NMDA
Postsynaptic Density
Na+/Ca2+
Na+
K+
K+
NMDA
NMDA
Non-NMDA
Non-NMDA
Postsynaptic Density

B

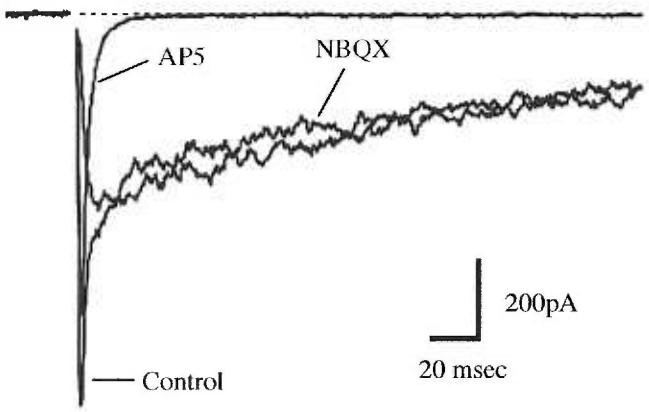
AP5
NBQX
200pA
20 msec
Control

Figure 2

A

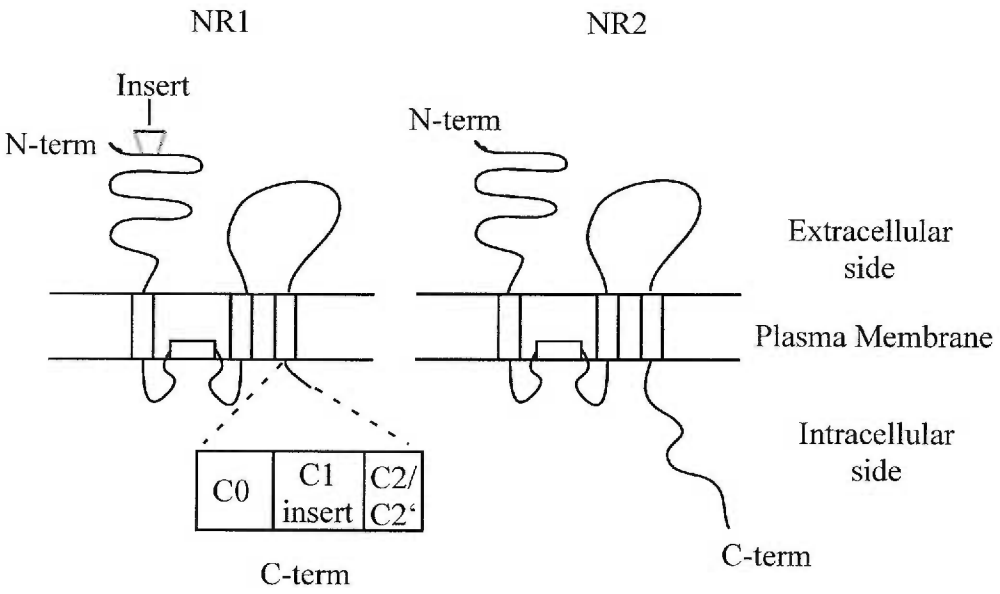
NR1
NR2
Insert
N-term
N-term
Extracellular side
Plasma Membrane
Intracellular side
C0
C1 insert
C2/ C2'
C-term
C-term

B

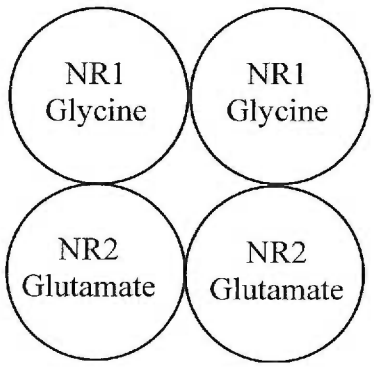
NR1 Glycine
NR1 Glycine
NR2 Glutamate
NR2 Glutamate

Figure 3

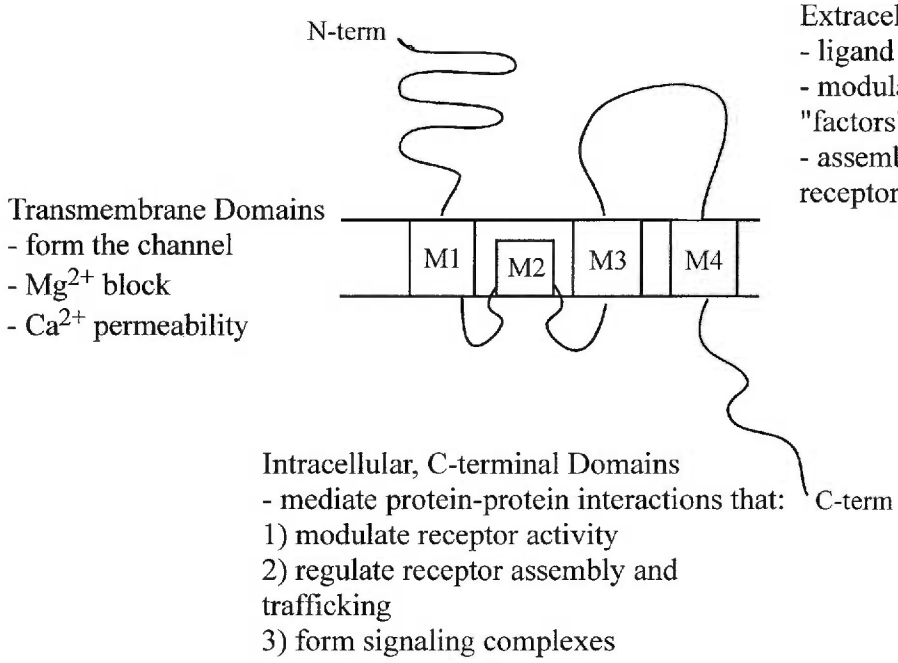
N-term
Extracellular Domains
- ligand binding
- modulation by extracellular "factors", e.g. zinc
- assembly of functional receptors
Transmembrane Domains
- form the channel
- Mg^{2+} block
- Ca^{2+} permeability
M1
M2
M3
M4
Intracellular, C-terminal Domains
- mediate protein-protein interactions that:
1) modulate receptor activity
2) regulate receptor assembly and trafficking
3) form signaling complexes
C-term

Chapter 1

Synaptic and Extrasynaptic NMDA Receptor NR2 Subunits in Cultured Hippocampal Neurons

Christopher G. Thomas, Ashleigh J. Miller, and Gary L. Westbrook

Vollum Institute, Oregon Health and Science University, Portland, OR 97239

Running Head: NR2 subunit Distribution in Cultured Hippocampal Neurons

Contact Information:

Gary L. Westbrook

Vollum Institute

OHSU L474

3181 SW Sam Jackson Park Rd

Portland, OR 97239

westbroo@ohsu.edu

Abstract

Early in development, neurons only express NR1/NR2B-containing NMDA receptors. Later, NR2A subunits are upregulated during a period of rapid synapse formation. This pattern is often interpreted to indicate that NR2A-containing receptors are synaptic and that NR2B-containing receptors are extrasynaptic. We re-examined this issue using whole-cell recordings in cultured hippocampal neurons. As expected, the inhibition of whole-cell currents by the NR2B-specific antagonist, ifenprodil, progressively decreased from 69.5 ± 2.4% (6 DIV) to 54.9 ± 2.6% (8 DIV), before reaching a plateau in the second week (42.5 ± 2%, 12-19 DIV). In $NR2A^{-/-}$ neurons, which express only NR1/NR2B-containing NMDA receptors, autaptic EPSCs (≥ 12 DIV) were more sensitive to ifenprodil and decayed more slowly than EPSCs in wild-type neurons. Thus NR2B-containing receptors were not excluded from synapses. We blocked synaptic NMDA receptors with MK-801 during evoked transmitter release, thus allowing us to isolate extrasynaptic receptors. Ifenprodil inhibition of the extrasynaptic population was highly variable in different neurons. Furthermore, extrasynaptic receptors in autaptic cultures were only partially blocked by ifenprodil, indicating that NR2A-containing receptors are not exclusively confined to the synapse. Extrasynaptic NR2A-containing receptors were also detected in $NR2A^{-/-}$ neurons transfected with full-length NR2A. Truncation of the NR2A C-terminus did not eliminate synaptic expression of NR2A-containing receptors. Our results indicate that NR2A- and NR2B-containing receptors can be located in either synaptic orextrasynaptic compartments.

Keywords: Synaptic, extrasynaptic, receptor targeting, postsynaptic density, protein-protein interactions.

Introduction

NMDA receptors are multimers of NR1/NR3 and NR2 subunits. The time- and tissue-specific expression of NR2 subunits affect channel properties as well as the distribution of NMDA receptors (Monyer et al. 1994). Expression of the NR2A subunit in the rodent CNS begins at 6-10 days postnatal (Monyer et al. 1994; Sheng et al. 1994; Zhong et al. 1994), a particularly dynamic period in synapse development. Before that point, hippocampal NMDA receptors are largely NR1/NR2B heterodimers, resulting in excitatory postsynaptic currents (EPSCs) that slowly deactivate and are strongly inhibited by NR2B-specific antagonists such as ifenprodil (Flint et al. 1997; Kew et al. 1998; Kirson and Yaari 1996; Li et al. 1998; Tovar and Westbrook 1999). NR2A can be incorporated into several subunit combinations including NR1/NR2A heterodimers and NR1/NR2A/NR2B heterotrimers, resulting in a developmental reduction in NR2B-specific antagonist sensitivity as well as an acceleration of the deactivation of NMDA receptor-mediated EPSCs. (Flint et al. 1997; Kew et al. 1998; Kirson and Yaari 1996; Li et al. 1998; Tovar and Westbrook 1999). Although NR2A subunits clearly contribute to synaptic NMDA receptors, the existing data does not completely support the idea that NR2A-containing receptors are exclusively synaptic and NR2B-containing receptors are exclusively extrasynaptic (Mohrmann et al. 2000; Stocca and Vicini 1998; Tovar et al. 2000; Townsend et al. 2003).

Recent experiments suggest that synaptic and extrasynaptic receptors may have distinct roles in synaptic plasticity, coupling to intracellular signaling cascasdes, and cell death (Hardingham et al. 2002b; Liu et al. 2004b; Massey et al. 2004). During synaptic development, NMDA receptors become clustered at synapses, but a population of extrasynaptic receptors remains (Cottrell et al. 2000; Pickard et al. 2000; Rosenmund et al. 1995). Synaptic clustering of NMDA receptors is in part controlled by intracellular protein-protein interactions with postsynaptic density proteins (Bolton et al. 2000; Scannevin and Huganir 2000). The sequence of trafficking, targeting, and anchoring of NMDA receptors remains an active area of investigation (Perez-Otano and Ehlers 2004; Wenthold et al. 2003). The underlying mechanisms for localization and signaling may involve differential binding of proteins to the cytoplasmic domains of NR2A and NR2B (Guillaud et al. 2003; Lavezzari et al. 2004; Sans et al. 2000).

We used whole-cell recordings in cultured hippocampal neurons to determine the NR2 subunit composition of synaptic and extrasynaptic receptors during development *in vitro*. We confirmed that NR2A-containing receptors are incorporated into synapses during development. However, the extrasynaptic population included both NR2B- and NR2A-containing receptors. Transfection of an NR2A C-terminal truncation mutant subunit into neurons from $NR2A^{-/-}$ mice demonstrated that the cytoplasmic domain was not essential for synaptic localization.

Materials and Methods

Cell Culture. Cell cultures were prepared from hippocampi of newborn wild-type or $NR2A^{-/-}$ mice. As previously described (Jahr and Stevens 1987), hippocampi were

removed, incubated with papain (Worthington, Lakewood, N.J.), then mechanically dissociated. Neurons (150,000 cells/dish) were plated onto a confluent layer of glia on glass coverslips (Fisher, Pittsburgh, PA). For single neuron (autaptic) cultures, cells (50,000 cells/dish) were plated onto glial microislands. Hippocampal glia were grown to confluency on coverslips (25 mm) coated with collagen (Cohesion, Palo Alto, CA) and poly-L-lysine (Sigma). For autapses, coverslips were coated with 0.15% agarose (Sigma, St. Louis, MO), then sprayed with a mixture of collagen, poly-D-lysine (BD Biosciences, Bedford, MA) and 17 mM acetic acid (Bekkers and Stevens 1991). For some experiments, 100 μM AP5 (Tocris, Ellisville, MO) was added to the culture medium from 4-6 DIV.

Genotyping. $NR2A^{-/-}$ mice were bred on a C57BL/6 wild-type background and genotyped using polymerase chain reaction (PCR) amplification of genomic DNA. As previously described (Tovar et al. 2000), tissue was incubated in proteinase K (0.5 mg/ml; GibcoBRL, Carlsbad, CA) at 55°C for ≥ 12 hours. Samples were centrifuged and genomic DNA was precipitated from supernatants by adding an equal volume of isopropanol. The precipitated DNA was pelleted by centrifugation, washed in ice cold 70% ethanol and allowed to dry. Genomic DNA was resuspended in TE buffer (10 mM Tris, 1 mM EDTA, pH 8.0) and added to the following PCR mixture: Mg^{2+} (2.15 mM), dNTPs (0.2 mM each), oligonucleotide primers (0.01 mg/ml each, *Taq* polymerase (2.5 units Promega, Madison, WI), reaction buffer (5 μL), and 2 μL of solubilized genomic DNA (50 μL final volume) in HPLC water. Two reactions were performed on each DNA sample. The first reaction used: *Primer 1*; 5'-TCTGGGGCCTGGTCTTCAACAATTCTGTGC-3'; *Primer 2*; 5'-

CCCGTTAGCCCGTTGAGTCACCCCT-3', and the *Neo Primer*; 5'-GCCTGCTTGCCGAATATCATGGTGGAAAAT-3'. The second reaction used *Primer 1*, the *Neo Primer*, and *Primer 3*: 5'-ATTCTTTGATAAATGCAATGATGGGGG-3'. Reaction products were run on 2% agarose gels and visualized using ethidium bromide. In the first set of reactions, DNA from NR2A$^{-/-}$ mice yielded 1553 and 418 base pair (bp) products whereas DNA from wild-type mice yielded a single 180 bp product. The 418 bp product represented the *neop1* gene insert. In the second set of reactions DNA from NR2A$^{-/-}$ mice yielded 1620 and 485 (*neo1p* insert) bp products whereas DNA from wild-type mice yielded a single 253 bp product. Gel purification and sequencing of the reaction products yielded the expected DNA sequences (data not shown).

Transfection. We transfected cell cultures at 6 DIV using the lipid-based Effectene kit (Qiagen USA, Valencia, CA). For most experiments, cultures were incubated in serum-free media for 2 hours before the reaction solution containing 0.5 μg of full-length NR2A or the truncation mutant (NR2A$_{stop844}$) subunit plasmid cDNA and 0.5 μg of EGFP plasmid cDNA was added to each culture. Transfections were stopped after 90 minutes by replacing the media with serum-containing media. Recordings from transfected neurons were made 1-3 days after transfection (7-9 DIV). For imaging, 0.5 μg of EGFP-tagged NR2A (GFP-NR2A) was cotransfected with 0.5 μg of carrier DNA (Gibco-BRL). NR2A, NR2A$_{stop844}$, and GFP-NR2A cDNA were inserted into pcDNA1/AMP provided by Stephen Heinemann (Salk Institute, La Jolla, CA). The EGFP construct was inserted into the JPA7 vector provided by Gary Banker (CROET, OHSU, Portland, OR).

Electrophysiology. Whole-cell voltage clamp recordings were made at a holding potential of -70 mV. The superfused extracellular bath solution contained (in mM): 162 NaCl, 2.4 KCl, 10 HEPES, 10 glucose, 1 $CaCl_2$, 0.0005 TTX (Alomone Labs, Jerusalem, Israel), 0.01 bicuculline methiodide (Sigma), 0.002 strychnine (Sigma), 0.1 glycine, pH 7.2, 320 mOsm. For autapses, TTX was omitted and calcium was increased to 2 mM. Patch pipettes (2-5 MΩ) were filled with (in mM): 145 Cs-gluconate, 1 $MgCl_2$, 10 HEPES, 1.1 EGTA, 5 CsBAPTA, pH 7.2, 310 mOsm. For autapses we used (in mM): 150 K-gluconate, 1.418 $CaCl_2$, 2 $MgCl_2$, 10 EGTA, 10 HEPES, 2 Na_2ATP, 0.2 GTP, pH 7.2, 310 mOsm. Quartz flow pipes for solution exchanges were placed 50-100 μm from the cell and mounted to a piezoelectric bimorph driven by a stimulus isolation unit (Winston Electronics, San Francisco, CA). Step depolarizations (+10 mV, 0.5 ms) were used to evoke autaptic EPSCs. Currents were recorded using an Axopatch 1C (Axon Instruments, Foster City, CA) amplifier and Axograph acquisition software. Currents were filtered at 2 kHz and digitized at 5 kHz.

Immunofluorescence. Four days after transfection, GFP-NR2A-transfected $NR2A^{-/-}$ neurons (10 DIV) were live stained (anti-GFP, rabbit, Molecular Probes, Eugene, OR, 1:200) in serum-free medium for 5 minutes at 37°C. Neurons were then washed in PBS solution containing 1 mM $MgCl_2$ and 0.1 mM $CaCl_2$, fixed in 4% paraformaldehyde and 4% sucrose in PBS for 20 min. at 37°C. Cells were then permeabilized in 0.3% Triton-X-100 in PBS for 5 min., blocked in 0.5% fish gelatin in PBS for 30 minutes, incubated in primary antibody (anti-Synapsin 1, mouse, Synaptic Systems, Goettingen, Germany, 1:500 in blocking solution) for 2-3 hours and then in secondary antibodies (goat anti-mouse Alexa A633, Molecular Probes, 1:1000 and biotinylated goat anti-

rabbit, Jackson ImmunoResearch Laboratories, West Grove, PA, 1:1000 in blocking solution) for 30 min., and finally incubated in Cy3 streptavidin (Jackson, 1:10000, in blocking solution) for 30 min.. All steps excluding live staining and fixation were performed at room temperature. A Leica DM-RXA (Bannockburn, IL) microscope equipped with a 63x, 132 N.A. Plan Apo objective and a Princeton Instruments Micromax (Trenton, N.J.) CCD camera were used for immunofluorescense imaging of stained neurons. Digital images were acquired and pseudocolored with MetaMorph (Universal Imaging, Buckinghamshire, UK) imaging software and prepared for presentation with Adobe Photoshop (San Jose, CA).

Data Analysis. Currents were analyzed with Axograph software (Axon Instruments). Ifenprodil inhibition was expressed as percent inhibition of the peak NMDA receptor-mediated current $(1-(I_{NMDA+Ifenprodil}/I_{NMDA}))$ x100. Miniature EPSC recordings were analyzed with a variable template function. The template was set up to detect AMPA receptor-mediated events that were 5-6 times greater than the standard deviation of the background noise. Each event was verified by eye and averaged with a minimum of 50 events per recording condition. Autaptic EPSCs and mEPSCs were averaged for each drug condition. Ifenprodil inhibition of EPSCs was expressed as percent inhibition of the NMDA receptor-mediated component, measured 10-20 ms after the beginning of an event. The decay of NMDA receptor-mediated autaptic EPSCs, recorded in the presence of NBQX, was fit with the sum of two exponentials and presented as a weighted average decay. Pooled data are presented as mean ± SEM. For statistical comparisons, paired and unpaired *t* tests or ANOVAs with subsequent Bonferroni/Dunn

test for multiple comparisons were used as appropriate. Statistical significance was set at $p < 0.05$.

Results

NR2A subunits are incorporated into NMDA receptors during synaptic maturation in vitro

We used the noncompetitive, NR2B-selective inhibitor, ifenprodil to examine the contribution of NR2A and NR2B subunits to whole-cell and synaptic currents. At a concentration of 3 μM, ifenprodil blocked 73.8 ± 2.4% of whole-cell NMDA-induced currents recorded in hippocampal neurons from $NR2A^{-/-}$ mice (n = 14, Figure 1A, 1B) that only express NR1/N2B heterodimeric NMDA receptors. This concentration of ifenprodil is the highest that can be used without affecting NR2A-containing receptors, and the degree of block we observed is consistent with block of NR1/2B recombinant receptors (Tovar and Westbrook 1999). NR2A expression develops as synaptic activity gradually increases during the first week *in vitro* (Monyer et al. 1994; Sheng et al. 1994). Thus to synchronize NR2A expression (Chavis and Westbrook 2001; Hoffmann et al. 2000), we blocked synaptic activity with AP5 (100 μM) between days 4 and 6 *in vitro*. Ifenprodil inhibited 69.5 ± 2.4% (n = 25) of the whole-cell current recorded in wild-type neurons at 6 DIV, consistent with prior evidence that early in development NMDA receptors are almost all NR1/NR2B heteromers. We were able to control NR2A expression to some extent between 4-6 days in culture by blocking NMDA receptors, but not completely. The slightly higher ifenprodil inhibition in $NR2A^{-/-}$ neurons than in wild-type neurons at 6 DIV presumably reflects a small amount of NR2A expression triggered by residual synaptic activity between days 4 and 6. Ifenprodil inhibition

decreased from 61.4 ± 2% (n = 29) at 7 DIV and 54.9 ± 2.6% (n = 26) at 8 DIV to 42.5 ± 2% (n = 21) in synaptically mature neurons (12-19 DIV). This is consistent with an increase in NR2A-containing receptors, but also indicates that both NR2A- and NR2B-containing receptors contribute to the whole-cell current even in synaptically mature cells.

Whole-cell currents include both synaptic and extrasynaptic components. To examine synaptic NMDA receptors, we evoked EPSCs in autaptic cultures. EPSCs in wild-type (12-19 DIV) and NR2A$^{-/-}$ neurons (12-19 DIV) had a fast AMPA receptor component followed by an AP5-sensitive NMDA receptor component (Figure 1C). Ifenprodil blocked 86.5 ± 5.7% (n = 4) of NR2A$^{-/-}$ EPSCs, demonstrating that NR1/2B receptors can be located at synapses after synaptic maturation. Ifenprodil inhibition was partial in wild-type neurons (55.8 ± 9.9%, n = 5), indicating NR2B-containing receptors are also present at wild-type synapses. NR1/2B receptors have much slower deactivations than NR1/2A receptors (Vicini et al. 1998). Thus as expected NMDA receptor-mediated EPSCs in wild-type neurons decayed significantly faster (435 ± 31 ms, n = 6) than in NR2A$^{-/-}$ neurons (723 ± 64 ms, n = 4; Figure 1D). However, the deactivation of wild-type EPSCs was still slower than NR1/2A EPSCs recorded in NR2B$^{-/-}$ hippocampal autapses (Tovar et al. 2000). This was not a result of separate populations of NR1/2A and NR1/2B receptors at wild-type synapses because the deactivation remained the same in control solution as it did in the presence of ifenprodil (Fig. 1C, right panel).

Isolation of extrasynaptic NMDA receptors

It is difficult to separate synaptic and extrasynaptic receptors in most preparations. However, extrasynaptic NMDA receptors can be studied in isolation in autapses by first irreversibly blocking synaptic NMDA receptors with MK-801 (Rosenmund et al. 1995). We developed an analogous protocol using high potassium-evoked release of glutamate to block synaptic NMDA receptors in multi-cell cultures. We first measured the whole-cell NMDA current (Fig. 2A, left panel). Then the cell was treated with a series of 10 or more whole-cell applications (500 ms) of potassium (90 mM), calcium (6 mM), and MK-801 (60 μM), in the presence of NBQX (5μM) until the current reached a plateau, (Figure 2A, middle panel). The residual current after 10 applications represented inward potassium current induced by the 90 mM K^+ solution. Subsequent application of NMDA revealed that the treatment irreversibly blocked 71 ± 3% (n = 12) of the NMDA current. Substitution of AP5 (100 μM) for MK-801 did not reduce subsequent whole-cell NMDA currents (4.7 ± 3.1%, n = 4), indicating that potassium treatment itself did not affect the NMDA current. The fraction of remaining NMDA current was similar to the extrasynaptic fraction previously reported in autapses (Rosenmund et al. 1995).

We recorded mEPSCs before and after MK-801 block to confirm that the protocol blocked all synaptic NMDA receptors (Figure 2B). The ensemble average mEPSC before MK-801 had an NMDA receptor-mediated component that was blocked by AP5 (Figure 2C, left panel). However, the NMDA receptor component was no longer present following MK-801 block (Fig. 2C, right panel, n = 6). The treatment protocol did not change the amplitude of the AMPA receptor–mediated mEPSCs or the

frequency of events suggesting that transmitter release was unaffected (Fig. 2D). Autaptic EPSCs, recorded before and after MK-801 also showed that the treatment protocol blocked synaptic NMDA receptors (data not shown). Thus the NMDA current remaining after MK-801 is only mediated by extrasynaptic receptors. We used this strategy to investigate the distribution of NR2A- and NR2B-containing receptors.

NR2A is present in extrasynaptic NMDA receptors

If NR2A-containing receptors are synaptic and NR2B-containing receptors are extrasynaptic then the extrasynaptic population should be highly sensitive to ifenprodil. In order to follow the distribution of newly expressed NR2A subunits during maturation, we measured ifenprodil inhibition of NMDA receptor currents before and after MK-801 treatment. As seen in Figure 1, ifenprodil inhibition of total whole-cell current, including both synaptic and extrasynaptic receptors, was less in synaptically mature neurons (43.4 ± 2.6 %, n = 14) than at 6 DIV (64.4 ± 3.6 %, n = 12; Figure 3B, left panels). The ifenprodil inhibition of the extrasynaptic population as measured following MK-801 treatment (Figure 3A, right panels) was highly variable between neurons. At 6 DIV, the ifenprodil inhibition of the extrasynaptic population was 63.8 ± 3.8 % (range 39-83, n = 12; Fig. 3A, top right). In synaptically mature neurons, the ifenprodil inhibition was 49.1 ± 3.5 % (range 19-61, n = 13), which was marginally greater than that for the total whole-cell current (Fig. 3A, lower panels). The variability in ifenprodil inhibition of the extrasynaptic population suggested that, at least in some cells, NR2A-containing receptors were extrasynaptic. Consistent with this idea, the total and extrasynaptic population of NMDA receptors in mature autapses showed similar

ifenprodil inhibition (Figure 3B). Before MK-801, the inhibition was 42.5 ± 6.9% (n = 4) compared to 37.5 ± 5.5% (n = 4) after blocking synaptic NMDA receptors. Furthermore, in inhibitory neuron autapses that lack any synaptic NMDA receptors, ifenprodil inhibition of this purely extrasynaptic population was 40.1 ± 5.1% (n = 9). Thus under several different experimental conditions, the ifenprodil sensitivity of the extrasynaptic population is less than predicted for NR1/NR2B receptors.

Transfected NR2A is incorporated into synaptic NMDA receptors of NR2A$^{-/-}$ neurons

The intracellular domains of NMDA receptors subunits contain protein interacting domains that are thought to influence their targeting, location, and function (Perez-Otano and Ehlers 2004; Wenthold et al. 2003). In order to examine the role of the cytoplasmic domain of NR2A in synaptic localization, we used NR2A$^{-/-}$ neurons as a background into which we introduced full-length or mutant recombinant NR2A subunits. We transfected NR2A$^{-/-}$ cultured neurons at 6 DIV with an N-terminally, EGFP-labeled NR2A (GFP-NR2A) subunit. Four days later (10 DIV), the neurons were live-immunostained for GFP, fixed, permeabilized, and immunostained for synaptophysin. Puncta representing cell-surface GFP-NR2A were scattered throughout the dendrites (Figure 4A, red pseudocolor). In these cultures containing both excitatory and inhibitory neurons, the presynaptic marker synaptophysin identified synapses some of which were co-localized with GFP-NR2A (Figure 4A). These results indicate that transfected NR2A subunits were functionally expressed at synapses.

To examine the synaptic receptors in the transfected neurons, we recorded mEPSCs in cells that had been transfected with full-length NR2A subunit cDNA. GFP-

NR2A has low fluorescent intensity, thus we cotransfected the neurons with EGFP as a screen. Ensemble average mEPSCs from mature wild-type (12-19 DIV), mature untransfected NR2A$^{-/-}$ (12-19 DIV), and NR2A-transfected NR2A$^{-/-}$ (7-14 DIV) neurons all had fast AMPA receptor-mediated components followed by a slow NMDA receptor-mediated component (Figure 4B). In each case, the slow component was completely blocked by AP5. The NR1/2B receptors of the NR2A$^{-/-}$ mEPSCs were more inhibited by ifenprodil (71.8 ± 6.2%, n = 8 cells) than either wild type neurons (57.3 ± 8.3%, n = 6 cells) or NR2A$^{-/-}$ neurons transfected with NR2A (24.1 ± 12.3%, n = 4). Thus transfected full-length NR2A subunits were successfully incorporated into functional synaptic NMDA receptors.

NR2A subunits lacking the cytoplasmic domain can be located at synapses

Steigerwald et al. (2000) reported that mice expressing a C-terminal truncation mutant of NR2A have less synaptic NMDA receptors. We tested the role of the NR2A C-terminus using NR2A$^{-/-}$ neurons transfected with either a full-length NR2A or a C-terminal truncation mutant, NR2A$_{stop844}$ (Figure 5). Using the protocol shown in Figure 3, we measured ifenprodil inhibition of the total whole-cell NMDA current and the isolated extrasynaptic component. Compared with ifenprodil inhibition of untransfected NR2A$^{-/-}$ neurons (73.79 ± 2.4%, n = 14), expression of either NR2A subunit significantly reduced inhibition both before and after MK-801 treatment. For neurons transfected with full-length NR2A ifenprodil inhibition was 32.8 ± 5.9%, (n = 9) before MK-801 treatment and 24.4 ± 5.6%, (n = 9) after the treatment. For neurons transfected with NR2A$_{stop844}$, ifenprodil inhibition was 56.2 ± 4.3% (n = 12) before MK-801

treatment and 53.9 ± 3.8% (n = 12) after the treatment. There was no effect on the average amplitude of the whole-cell current ($NR2A^{-/-}$, 4.2 ± 1.1 nA, n = 14; $NR2A^{-/-}$ + NR2A, 6.6 ± 0.9 nA, n = 9; $NR2A^{-/-}$ + $NR2A_{stop844}$, 6.6 ± 1.2 nA, n = 12). Thus transfected NR2A subunits lacking the C-terminal domain can be incorporated into synaptic as well as extrasynaptic NMDA receptors. Consistent with this idea, ifenprodil inhibition of the ensemble average mEPSC from $NR2A^{-/-}$ neurons transfected with $NR2A_{stop844}$ was 22.0 ± 5.9% (n = 7).

Although the NR2A C-terminal truncation mutant was expressed at synapses, the surface expression of this construct appeared to be less than the full-length construct because whole-cell currents in $NR2A_{stop844}$-transfected neurons were significantly more sensitive to ifenprodil than those transfected with full-length NR2A. The vector for both constructs was the same, suggesting that truncation of the C-terminus affects receptor trafficking.

Discussion

We re-examined the NR2 subunit composition of synaptic and extrasynaptic NMDA receptors using cultured hippocampal neurons. Our results suggest that NR2A- and NR2B-containing receptors are not exclusively segregated into synaptic and extrasynaptic compartments. This conclusion was supported by analysis of the extrasynaptic complement of NMDA receptors in whole-cell currents, analysis of miniature and evoked EPSCs, and transfection of NR2A constructs into $NR2A^{-/-}$ neurons.

Validity of our approach

Our analysis relied on comparing the ifenprodil inhibition of whole-cell NMDA receptors before and after irreversible block of synaptic receptors with MK-801. The existence of triheteromeric receptors containing NR2A and NR2B (Sheng et al. 1994; Tovar and Westbrook 1999) complicates the analysis of NMDA receptor subunit composition based on selective NR2A and NR2B antagonists. We used ifenprodil because it has been characterized on NR1/2B as well as NR1/2A/2B receptors, and involves binding of the antagonist to two NR2B subunits for full inhibition (Hatton and Paoletti 2005; Kew et al. 1998; Tovar and Westbrook 1999). Even on NR1/2B receptors, ifenprodil at selective concentrations only blocks about 75-80% of NR1/2B current due to its noncompetitive kinetics. Using this degree of block as a reference, most whole-cell current or EPSCs in mature hippocampal neurons are partially inhibited by ifenprodil (Tovar and Westbrook 1999) reflecting the contribution of NR2A-containing receptors.

It is also essential to our analysis that we were able to isolate a pure population of extrasynaptic receptors. For whole-cell recording, we used a modified protocol based on irreversible block of synaptic NMDA receptors by MK-801 following evoked release (Rosenmund et al. 1995). The protocol we used eliminated the NMDA receptor component of mEPSCs as well as the evoked EPSC in autaptic neurons without affecting transmitter release, confirming that the remaining whole-cell NMDA responses were exclusively mediated by extrasynaptic NMDA receptors. The high potassium stimulation could have resulted in some spillover to extrasynaptic receptors,

but this would not affect our interpretations of the remaining extrasynaptic receptor current.

We used transfection of NR2A constructs into NR2A$^{-/-}$ neurons to examine whether the cytoplasmic domain was essential for the presence of NR2A-containing receptors at synapses. Inappropriate localization due to overexpression is always a concern with such experiments. However, the surface expression of NMDA receptors is limited by endogenous NR1, and the whole-cell current amplitudes were not increased in transfected neurons. In fact the surface expression of the truncation mutant was less than the full-length construct. Thus it seems unlikely that overexpression was the reason that NR2A subunits lacking cytoplasmic domains were present in synapses. We cannot exclude that receptors containing some exogenous NR2 subunits were inappropriately expressed in extrasynaptic locations. However, NR2A-containing receptors were also present in extrasynaptic receptors of wild-type neurons.

The distribution of NR2-containing receptors

Our results agree with some aspects of prior studies on NMDA receptor subunit distribution, but not with others. Specifically, the expression of both synaptic and extrasynaptic receptors early in cell culture consisted of NR1/2B receptors (Li et al. 1998; Tovar and Westbrook 1999). Also consistent with prior data, was that soon after synaptic maturation began NR2A-containing receptors appeared and contributed to synaptic responses. However, the consensus breaks down over whether NR2B-containing receptors can be expressed at synapses and whether NR2A-containing receptors can be expressed in extrasynaptic locations. Both of these occurred in our

experiments. It is perhaps not surprising that NR2B-containing receptors are expressed at synapses in NR2A$^{-/-}$ neurons, an effect that could be attributed to compensation. However, miniature NMDA-receptor mediated EPSCs disappear during development in collicular neurons (Townsend et al. 2003), suggesting that compensation does not occur in that preparation. There is strong evidence that NR2B subunits contribute to triheteromeric synaptic receptors in wild type neurons (Kew et al. 1998; Luo et al. 1997; Sheng et al. 1994; Tovar and Westbrook 1999). However, triheteromeric receptors, which are partially sensitive to NR2B-selective antagonists, have not been seen in all cases (Stocca and Vicini 1998).

In occipital cortex cultures, Mohrmann et al. (2000) reported the presence of extrasynaptic NR2A-containing receptors whereas such receptors were not detectable in mature autapic hippocampal cultures (Tovar and Westbrook 1999). Our results indicated that the expression of NR2A-containing receptors in the extrasynaptic population was variable between cells. Although the latter result suggests that NR2A receptors are not exclusively synaptic, it also suggests that their presence may be regulated. There are several possible explanations for these apparent discrepancies including differences in the developmental stage of the neurons or neuron-specific expression patterns depending on the presynaptic inputs (Gottmann et al. 1997; Ito et al. 2000).

The NR2A intracellular C-terminal domain

The intracellular domains of ionotropic glutamate receptor subunits provide binding motifs for many interacting proteins that function in the trafficking and

signaling of receptor complexes (Wenthold et al. 2003). Interactions between the C-terminal domains of NMDA receptor subunits and intracellular proteins are thought to control the synaptic and extrasynaptic localization of NMDA receptors (Perez-Otano and Ehlers 2004). The intracellular domains of NR2A and NR2B can differentially interact with proteins involved in trafficking and anchoring, thus providing a potential mechanism for differential distribution of NR2A- and NR2B-containing receptors (Wenthold et al. 2003). Consistent with an important role of the NR2A cytoplasmic domain in synaptic localization, Steigerwald et al. (2000) reported smaller NMDA receptor-mediated EPSCs and less clustering of receptors at synapses in hippocampal neurons from transgenic mice expressing an NR2A truncation mutant. However, they also noted an overall decrease in total NR2A expression.

Given this evidence, it was somewhat surprising to us that truncated NR2A subunits were present in synaptic NMDA receptors of transfected NR2A$^{-/-}$ neurons. NMDA current amplitudes in transfected neurons were not increased compared to wild-type neurons suggesting that overexpression did not cause inappropriate targeting to the synapse. Prybylowski et al. (2002) also did not see increased synaptic current when NR2A was overexpressed in wild-type cerebellar granule cells. Our results by no means eliminate the possibility that the intracellular domain of NR2 subunits influences targeting because both NR1 and NR2B subunits were intact and therefore NR1/NR2A heterodimeric or NR1/N2A/NR2B heterotrimeric receptors could be compensatory.

Perhaps more interestingly, truncation of the cytoplasmic domain reduced the surface expression of NR2A-containing receptors as also was observed by Steigerwald et al. (2000). This suggests that the cytoplasmic domain is important in receptor

trafficking. For example, elimination of the PDZ binding motif, that occupies the last four amino acids (ESDV) of the NR2A and NR2B C-termini (Kim and Sheng 2004), reduces the contribution of NR2A and NR2B to synaptic NMDA receptors (Barria and Malinow 2002). In addition, NR2A and NR2B may be trafficked differently (Guillaud et al. 2003; Lavezzari et al. 2004; Sans et al. 2000).

NR2A, NR2B, synaptic and extrasynaptic

The categorization of NR2A-containing receptors as synaptic and NR2B-containing receptors as extrasynaptic has taken on additional significance because extrasynaptic receptors appear to have important functions. For example, extrasynaptic receptors have been reported to influence synaptic plasticity (Liu et al. 2004; Massey et al. 2004) and neuronal cell death (Hardingham et al. 2002). These distinctions may involve not only different access to released glutamate, but also different intracellular signaling cascades. Our results indicate that the segregation of NR2A and NR2B is not absolute. Although the NR2-selective antagonists are handy tools, they cannot always be equated with selective block of synaptic or extrasynaptic receptors. Thus separation of these receptor populations using methods such as MK-801 block may be preferable.

Acknowledgements

This work was supported by National Institutes of Health Grant MH46613 (G.L.W.). We thank Lindsay Grimes, Forrest Davis and Robert Mouton for preparation of hippocampal cell cultures, Dr. Masayoshi Mishina for the $NR2A^{-/-}$ mouse, Drs. Bryce Vissel and Stephen Heinemann for NMDA receptor clones, Dr. Stephanie Kaech, Dr. Michael A. Silverman, Dr. Gary Banker, Sonal Das and Greta Glover for the EGFP

clone and for advice with immunocytochemistry, and Drs. Johannes J. Krupp and Kenneth R. Tovar for useful comments.

Figure Legends

Figure 1. NR2A subunits are incorporated into NMDA receptors during synaptic maturation *in vitro*. A: We recorded responses to 500 ms whole-cell applications of NMDA (100 μM) or NMDA and ifenprodil (3 μM) from NR2A$^{-/-}$ (*left*) and from wild-type neurons at 6 DIV (*middle*) and ≥ 12 DIV (*right*). Wild-type neurons were pretreated with AP5 (100 μM) for 48 hours between 4-6 DIV to reduce NR2A expression. As a result, ifenprodil inhibition of wild-type neurons at 6 DIV was similar to that of NR2A$^{-/-}$ neurons that express only NR1/NR2B NMDA receptors. B: Ifenprodil inhibition of neurons progressively declined due to increased NR2A expression, but reached a plateau between 12-19 DIV (NR2A$^{-/-}$, n = 16; wild-type 6 DIV, n = 21; 7 DIV, n = 29; 8 DIV, n = 26; 12-19 DIV, n = 21; ANOVA with Bonferroni post-hoc test, $p < 0.01$; * = different than NR2A$^{-/-}$; † = different than 6 DIV wild-type). C: Autaptic EPSCs from synaptically mature (≥ 12 DIV) NR2A$^{-/-}$ (*left*) and wild-type (*right*) neurons were recorded in control solution and following perfusion with AP5 (100 μM) or ifenprodil (3 μM). The slow component was blocked by AP5. EPSCs in wild-type neurons were less inhibited by ifenprodil than in NR2A$^{-/-}$ neurons, indicating that NR2A subunits are incorporated into synaptic NMDA receptors. D: Normalized average NMDA receptor-mediated autaptic EPSCs recorded from mature NR2A$^{-/-}$ and wild-type neurons in the presence of 5 μM NBQX. Decay currents were fitted with the sum of two exponentials. The weighted average of time constants for the

wild-type EPSCs decayed significantly faster (435 ms, n = 6) than $NR2A^{-/-}$ EPSCs (723 ms, n = 4).

Figure 2. MK-801 blocked synaptic NMDA receptors during potassium-induced release. A: Whole-cell NMDA receptor responses recorded from a synaptically mature wild-type neuron before (*left*) and after (*right*) repeated applications of a high K^+/MK-801 solution (90 mM K^+, 60 μM MK-801, 6 mM $CaCl_2$, 5 μM NBQX, *middle*). MK-801 block reduced the whole-cell NMDA receptor current in this neuron by 80%. The time-independent residual current after the 15th application reflects inward K^+ leak current in the presence of 90 mM K^+. B: Miniature EPSCs recorded from a wild-type neuron in control (*top*) or AP5 (100 μM, *bottom*), before (*left*) and after (*right*) the synaptic block protocol. C: Ensemble average mEPSCs from the cell shown in panel B had a slow-decaying, AP5-sensitive component (*left*) that was blocked by the high K^+/MK-801 treatment (*right*). D, *Left Panel*: NMDA receptor amplitudes, measured over a 10-20 ms interval of the ensemble mEPSC were eliminated by synaptic block with MK-801 (paired *t* test, $p < 0.005$). However the synaptic block protocol had no effect on the amplitude or the frequency of the AMPA receptor component of mEPSCs recorded in the presence of AP5 (n = 7).

Figure 3. The ifenprodil inhibition of extrasynaptic NMDA receptors was variable. A: Representative traces of whole-cell responses to NMDA (100 μM) or NMDA and ifenprodil (3 μM) recorded before (*left traces*) and after (*right traces*) blocking synaptic receptors with high K^+/MK-801 from 6 DIV (*top traces*) and synaptically mature

(*bottom traces*) wild-type neurons that had been chronically treated with AP5 (100 μM) for 48 hours between 4-6 DIV. Dashed lines compare ifenprodil inhibition before and after blocking with MK-801. B: Ifenprodil inhibition was recorded in synaptically mature autapses before (*left traces*) and after (*right traces*) blocking synaptic receptors with MK-801 during action potential-evoked transmitter release. The ifenprodil inhibition of extrasynaptic receptors (*top right traces)* in 6 DIV cells was similar to inhibition of the total population of receptors recorded before MK-801 block (*top left traces*). In contrast, the ifenprodil inhibition of extrasynaptic receptors recorded in synaptically mature neurons varied regardless of the way transmitter release was evoked during MK-801 block, indicating that extrasynaptic receptors may contain NR2A subunits.

Figure 4. Exogenous NR2A subunits are incorporated into synaptic NMDA receptors of transfected $NR2A^{-/-}$ neurons. A1& A2: Dendrites from two different $NR2A^{-/-}$ neurons (10 DIV) that were transfected at 6 DIV with N-terminally GFP-labeled NR2A cDNA (GFP-NR2A), live-stained with an anti-GFP antibody (*red*), fixed, permeabilized, and then counterstained with an anti-synapsin antibody (*green*). Arrows indicate examples of co-localization of cell-surface GFP-NR2A with synapsin. In each cell there were more GFP than anti-GFP puncta, suggesting that GFP-NR2A subunits were located both on the cell surface and in the cytoplasm (data not shown). B: Ensemble average mEPSCs recorded in the presence of control solution (*black*), AP5 (100 μM, *blue*), and ifenprodil (3 μM, *red*) from a 15 DIV wild-type neuron (*left panel*), a 12 DIV $NR2A^{-/-}$ neuron (*middle panel*), and a 14 DIV $NR2A^{-/-}$ neuron transfected with NR2A at 6 DIV

(*right panel*). Dashed lines indicate the 10-20 ms where NMDA receptor amplitudes were measured. Ifenprodil inhibition of the NR2A-transfected $NR2A^{-/-}$ neuron (57% inhibition) was less than that seen for the $NR2A^{-/-}$ neuron (82%) and similar to that for the wild type neuron (34%).

Figure 5. C-terminally truncated NR2A subunits are present in synaptic receptors of transfected $NR2A^{-/-}$ neurons. A: Neurons (7-9 DIV) from $NR2A^{-/-}$ mice were transfected at 6 DIV with either full-length NR2A (*top*) or the C-terminal truncation mutant, $NR2A_{stop844}$ (*bottom*). Representative traces of whole-cell responses to NMDA (100 μM) or NMDA and ifenprodil (3 μM) recorded before (*left*) and after (*right*) blocking synaptic receptors with high K^+/MK-801. B: Average ifenprodil inhibitions recorded, pairwise, before (*black panels*) and after (*grey panels*) MK-801 block from the transfected $NR2A^{-/-}$ neurons shown in A. Transfection of both types of subunits significantly reduced the ifenprodil inhibition of $NR2A^{-/-}$ neurons (*data not shown*). The ifenprodil inhibition of extrasynaptic receptors (*right traces*) from $NR2A_{stop844}$-transfected cells was the same as the total population (*left traces*), indicating that the subunit was present in synaptic and extrasynaptic receptors. Ifenprodil inhibited currents from $NR2A_{stop844}$-transfected neurons more than it did for those transfected with full-length NR2A, indicating that the truncation mutant was not incorporated into functional NMDA receptors as much as the full length subunit. Data represents averages ± SEM ($NR2A^{-/-}$ + NR2A, n = 9; $NR2A^{-/-}$ + $NR2A_{stop844}$, n = 12; ANOVA with Bonferroni/Dunn post-hoc test $p < 0.01$, † = different than $NR2A^{-/-}$ + NR2A before synaptic block; paired *t* test $p < 0.05$, * = different than before synaptic block.).

Figure 1

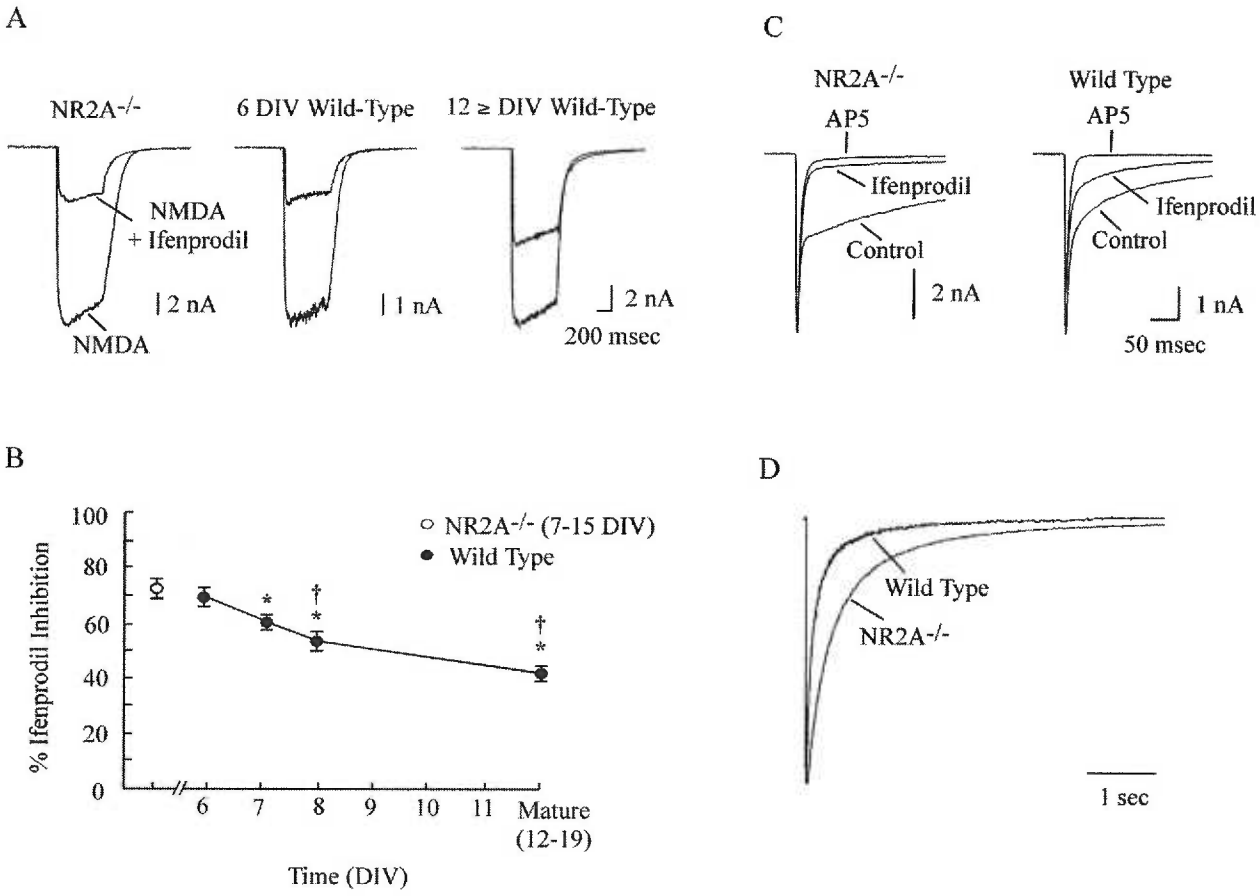
A
NR2A-/-
6 DIV Wild-Type
12 ≥ DIV Wild-Type
NMDA
+ Ifenprodil
2 nA
NMDA
1 nA
2 nA
200 msec
B
% Ifenprodil Inhibition
100
80
60
40
20
0
6
7
8
9
10
11
Mature
(12-19)
Time (DIV)
NR2A-/- (7-15 DIV)
Wild Type
C
NR2A-/-
AP5
Ifenprodil
Control
2 nA
Wild Type
AP5
Ifenprodil
Control
1 nA
50 msec
D
Wild Type
NR2A-/-
1 sec

Figure 2

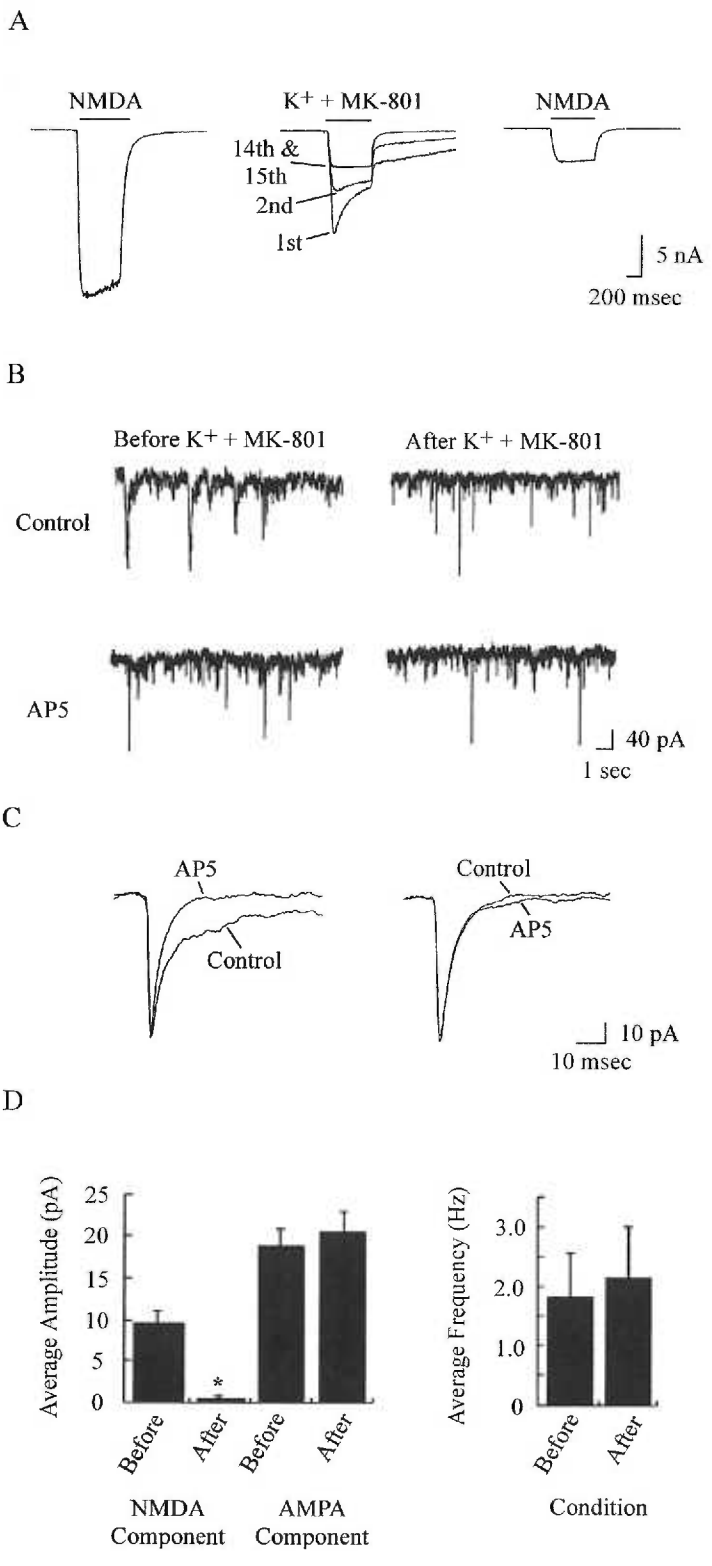
A
NMDA
K+ + MK-801
NMDA
14th &
15th
2nd
1st
5 nA
200 msec
B
Before K+ + MK-801
After K+ + MK-801
Control
AP5
40 pA
1 sec
C
AP5
Control
Control
AP5
10 pA
10 msec
D
Average Amplitude (pA)
25
20
15
10
5
0
*
Before
After
Before
After
NMDA Component
AMPA Component
Average Frequency (Hz)
3.0
2.0
1.0
0
Before
After
Condition

Figure 3

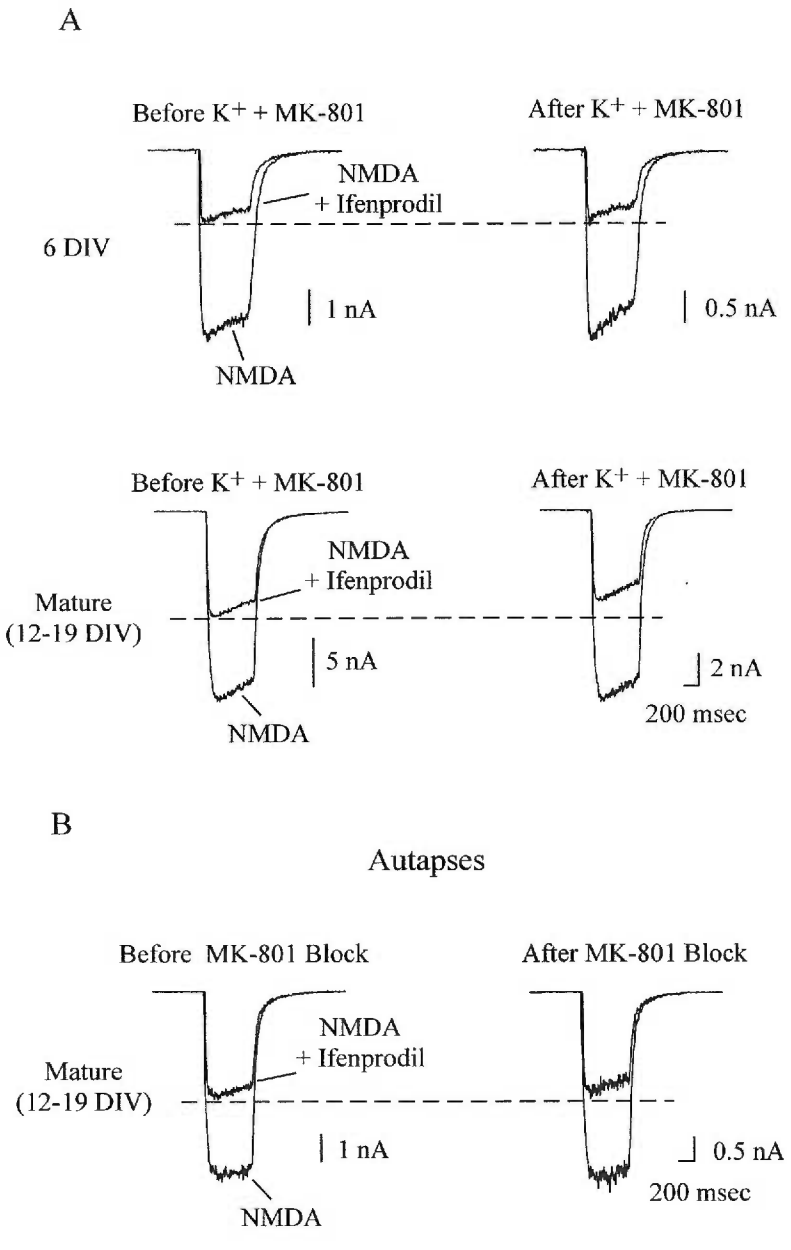
A
Before K+ + MK-801
After K+ + MK-801
NMDA
+ Ifenprodil
6 DIV
1 nA
0.5 nA
NMDA
Before K+ + MK-801
After K+ + MK-801
NMDA
+ Ifenprodil
Mature
(12-19 DIV)
5 nA
2 nA
200 msec
NMDA
B
Autapses
Before MK-801 Block
After MK-801 Block
NMDA
+ Ifenprodil
Mature
(12-19 DIV)
1 nA
0.5 nA
200 msec
NMDA

Figure 4

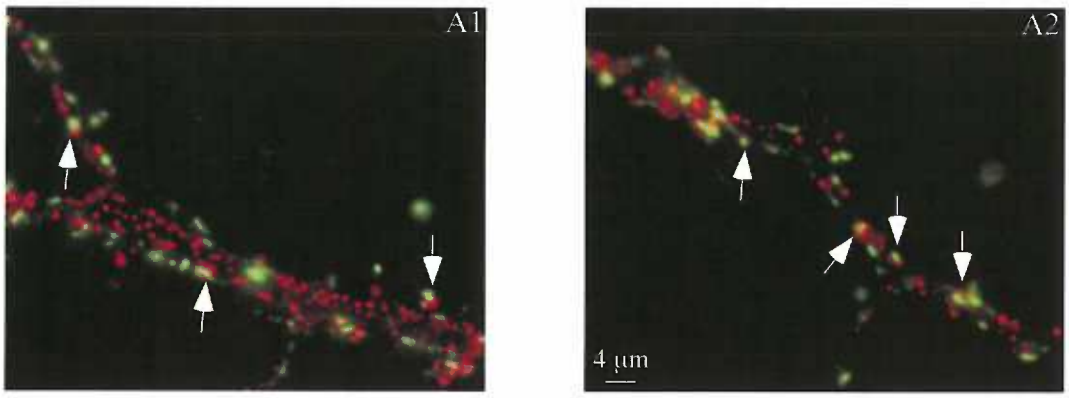

B

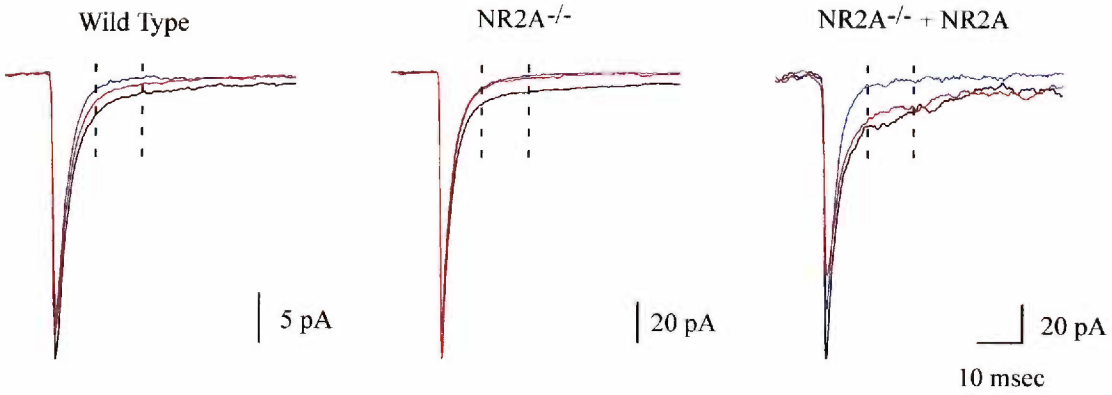

Figure 5

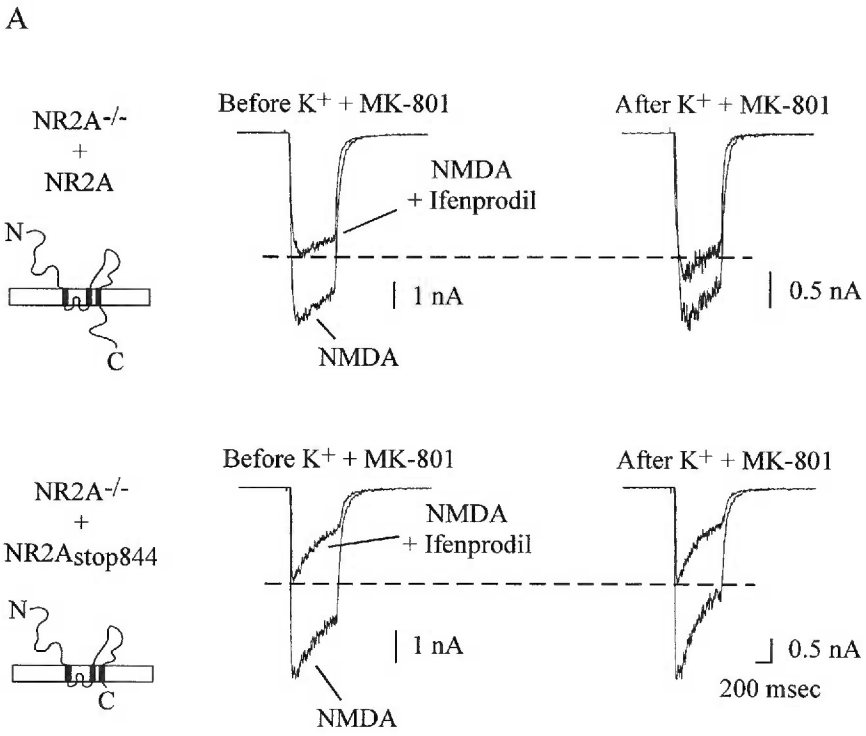
A
NR2A-/-
+
NR2A
N
C
Before K+ + MK-801
After K+ + MK-801
NMDA
+ Ifenprodil
1 nA
0.5 nA
NMDA
NR2A-/-
+
NR2Astop844
N
C
Before K+ + MK-801
After K+ + MK-801
NMDA
+ Ifenprodil
1 nA
0.5 nA
200 msec
NMDA

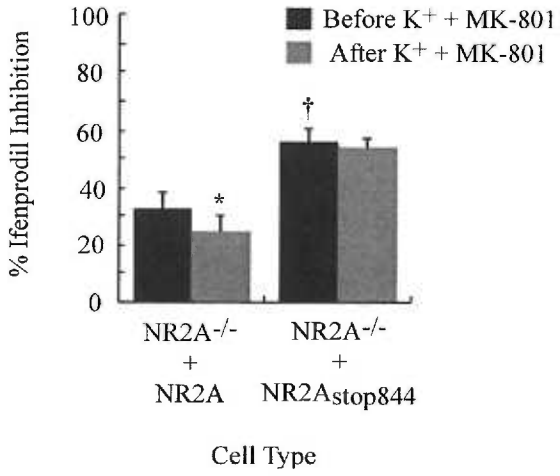
B
% Ifenprodil Inhibition
100
80
60
40
20
0
Before K+ + MK-801
After K+ + MK-801
*
†
NR2A-/-
+
NR2A
NR2A-/-
+
NR2Astop844
Cell Type

Chapter 2

Probing NMDA Receptor Desensitization with the Substituted-Cysteine Accessibility Method

Christopher G. Thomas[1], Johannes J. Krupp[2], Elena E. Bagley[3], Reginald Bauzon[4], Stephen Heinemann[5], Bryce Vissel[6], and Gary L. Westbrook[1]

[1]Vollum Institute, Oregon Health and Science University, Portland, OR 97239, U.S.A.

[2]AstraZeneca R&D Södertälje, B209, 15185 Södertälje, Sweden

[3]Pain Management Research Institute at Royal North Shore Hospital, The University of Sydney, NSW 2006, Australia

[4]3M Parmaceuticals, 3M Center, Building 0275-02-W-14, St. Paul, MN 55144-1000, U.S.A.

[5]The Salk Institute, 10010 North Torrey Pines Rd., La Jolla, California 92037, U.S.A.

[6]Neurobiology Research Program, Garvan Institute of Medical Research, 384 Victoria Street, Darlinghurst NSW 2010, Australia

Contact:

Gary L. Westbrook

Vollum Institute

Oregon Health and Science University, L474

3181 SW Sam Jackson Park Road

Portland, OR 97239

westbroo@ohsu.edu

Abstract

Several forms of macroscopic NMDA receptor desensitization affect the amplitude and duration of postsynaptic responses. In addition to its functional significance, desensitization provides one means to examine the conformational coupling of ligand binding to channel gating. Segments flanking the ligand-binding domain in the extracellular N-terminus of the NMDA receptor NR2 subunit influence the glycine-independent form of desensitization. The NR2A pre-M1 region, the linker between the glutamate binding domain and the channel pore, plays a critical role in desensitization. Thus we used the substituted-cysteine accessibility method to scan the accessibility of residues in the pre-M1 region and the first transmembrane domain (M1) of NR2A. Cysteine mutants were expressed with NR1 in HEK293 cells and assayed by whole-cell recording. With activation of the receptor by glutamate and glycine, only a single residue, V557C, located at the beginning of M1 was irreversibly blocked by the methanethiosulfonate derivative, MTSET. The NR2 ligand, glutamate, was insufficient on its own to induce modification of V557C by MTSET, suggesting that the change in accessibility required channel gating. The rate of MTSET modification of the homologous residue on NR1 (NR1-1a$_{I562C}$/NR2A) was much slower than V557C. We also substituted cysteine in the V557 site of mutant subunits that exhibit either enhanced or reduced desensitization. Modification by MTSET correlated with the degree of desensitization for these subunits suggesting that V557C is a sensitive detector of desensitization gating.

Introduction

The kinetics of NMDA receptors play an important role in shaping postsynaptic responses (Jones and Westbrook 1996; Lester and Jahr 1992; Qian and Johnson 2002). Although intrinsically silent, desensitized states can have significant actions on receptor gating (Jones and Westbrook 1996). Depending on the kinetics, desensitization can either accelerate or prolong the duration of a synaptic response. NMDA receptor channels are thought to desensitize directly from the closed, agonist bound state (Colquhoun and Hawkes 1995), thus glycine-independent desensitization represents a separate closed, bound conformation. This form of desensitization contributes to the decay of EPSCs and reduces NMDA receptor mediated responses during high frequency synaptic stimulation (Lester and Jahr 1992). Thus understanding the conformational changes associated with desensitization is ultimately important for understanding synaptic signaling.

NMDA receptors are tetramers comprised of two glycine-binding NR1 and two glutamate binding NR2 (A-D) subunits, possibly aligned in a 1-1-2-2 order (Clements and Westbrook 1991; Inanobe et al. 2005; Schorge and Colquhoun 2003). In some cell types NR3 subunits can be incorporated into NMDA receptors (Chatterton et al. 2002). The topology of NMDA receptor subunits consists of a large, N-terminal extracellular domain, four hydrophobic domains (M1-M4), and a cytoplasmic C-terminal domain (Mayer and Armstrong 2004; Wollmuth and Sobolevsky 2004). M2 is a reentrant P loop that lines the channel. The first 400 amino acids of the N-terminal domain are homologous to the leucine/isoleucine/valine-binding protein (LIVBP-like domain) followed by the agonist-binding S1 domain, and a short stretch of amino acids linking

the S1 and M1 domains - the pre-M1 region. Based on crystal structures of AMPA receptor subunits, ligand-binding sites of NMDA receptors operate like two lobes of a clamshell composed of the S1 domain on the N-terminal domain, and the S2 domain in the extracellular loop between M3 and M4 (Mayer and Armstrong 2004; Wollmuth and Sobolevsky 2004). A short segment linking M3 with the S2 domain is highly conserved among ionotropic glutamate receptors and influences channel gating (Jones et al. 2002; Kohda et al. 2000). Recent crystal structures have confirmed a clamshell arrangement for the glycine-binding pocket of the NR1 subunit (Furukawa and Gouaux 2003). Studies using the substituted-cysteine accessibility method (SCAM) on NR1 and NR2C subunits suggest that the structure of the pore resembles an inverted potassium channel, with a large extracellular vestibule surrounding the pore (Beck et al. 1999; Kuner et al. 2003). It has also been suggested that the extracellular vestibule is involved in activation and desensitization (Sobolevsky 1999; Sobolevsky et al. 1999). However little is known about the conformational changes that couple ligand binding to channel gating.

Kinetic models indicate that when bound by two molecules of glutamate and two molecules of glycine, NMDA receptor channels have two main options (other than unbinding): they can open or desensitize. The glycine-independent form of NMDA receptor desensitization is prominent in receptors containing the NR2A or NR2B subunit. Sobolevsky et al. (1999) proposed a physical model in which glycine-independent desensitization occurs because the channel contains a desensitization "gate" that is physically distinct from the activation "gate" (Sobolevsky et al. 1999). However, mutations in several regions of the NR2A subunit reduce or eliminate

desensitization in NR1/NR2A-containing receptors. These regions include the LIVBP-like domain, the pre-M1 region, the lurcher site in the third transmembrane domain, and a methionine (Met^{823}) in the fourth transmembrane domain (Kohda et al. 2000; Krupp et al. 1998; Meddows et al. 2001; Villarroel et al. 1998; Zheng et al. 2001). Similar results have been obtained by introducing mutations in the P-loop (Asn^{598}) or the lurcher site of NR1 (Chen et al. 2004; Kohda et al. 2000). The pre-M1 region of NR2A is a particularly attractive candidate for coupling ligand binding to channel gating because it links the glutamate-binding S1 domain to the channel. Studies showing that the pre-M1 region influences desensitization are consistent with this idea (Krupp et al. 1998; Sobolevsky et al. 2002; Villarroel et al. 1998).

We used substituted-cysteine mutagenesis to screen the accessibility of amino acids located in and around the pre-M1 region. Cysteine-substituted NR2A subunits were coexpressed in HEK293 cells with NR1. Whole-cell recordings were used to determine the accessibility of the substituted cysteines. Of the residues screened, MTS reagents modified two mutant NR2A subunits: $NR2A_{a548c}$ and $NR2A_{v557c}$. $NR2A_{v557c}$ modification required the presence of glutamate and glycine, thus it detected channel gating. Using modified NR2 subunits with varying amounts of desensitization, we found that the accessibility of V557C correlated with desensitization.

Materials and Methods

Molecular biology. All cDNAs encoding NMDA receptor subunits were cloned in pCDNA1/amp (Invitrogen, Carlsbad, CA). Clones used were NR2A (accession no. D13211; Ishii et al. 1993) and NR1-1a (accession no. U0826; Hollmann et al. 1993).

The NR1-1a$_{stop838}$ (Krupp et al. 1998) and NR2A$_{stop844}$ (Krupp et al. 2002) truncation mutants and NR2 chimeras, 2C$_0$A, AD1, and D001/AD1 have been described (Krupp et al. 1998). Point mutants were generated using gene splicing by overlap extension PCR with Pfu Polymerase (Stratagene, La Jolla, CA; Horten et al. 1989). DNAs generated by PCR were sequenced. Amino acids (aa) are numbered in accordance with (Ishii et al. 1993). Lymphocyte CD4 receptor cDNA was cloned in a JPA vector kindly provided by Dr. John Adelman (Vollum Institute).

Cell culture and transfection. HEK293 cells (ATCC, Manassas, VA or Invitrogen) grown in DMEM (Invitrogen), 10% heat-inactivated fetal calf serum (Hyclone, Logan, UT), 3 mM kynurenic acid (Sigma, St. Louis, MO), 1% glutamine, and 1% penicillin-streptomycin (Invitrogen; 37°C, 5% CO_2), were plated onto 35 mm, polylysine-coated glass cover slips 3-6 hours before transfection. Cells were transfected for 12-18 hours in the presence of kynurenic acid and DL-AP5 (1 mM, Tocris, Ballwin, MO) using the Ca^{2+}/phosphate method (Invitrogen) at an NR1:NR2:CD4 cDNA ratio of 4:4:1. Alternatively we used the Polyfect method (Qiagen, Valencia, CA) for 6-12 hours at an NR1:NR2:CD4 cDNA ratio of 8:8:1. We stopped transfections by replacing the media with fresh media containing AP5 and FUDR (0.2 mg/ml 5'-fluoro-2-deoxyuridine and 0.5 mg/ml uridine, Sigma). Anti-CD4 receptor-coated beads (Dynal, Oslo, Norway) were used to identify transfected cells.

Electrophysiology. We made whole-cell voltage-clamp recordings 12-48 hours after transfections. The recording chamber was continuously superfused at room temperature (~20°C) with extracellular solution containing (mM): NaCl 162, KCl 2.4, HEPES 10, Glucose 10, $CaCl_2$ 1 (pH 7.2, NaOH; 325 mOsm). Patch pipetttes (2-5 MΩ) were pulled

from thin-walled borosilicate glass (TW150F-6; World Precision Instruments, Sarasota, FL) and filled with (mM) $CsCH_4SO_3$ 115.5, HEPES 10, $MgCl_2$ 6, Na_2ATP 4, phosphocreatine 20, creatine phosphokinase 50 U/ml, leupeptin 0.1, BAPTA 10, $CaCl_2$ 1 (pH 7.2, CsOH; 310-320 mOsm). Where noted, the intracellular solution contained 0.1 mM EGTA and no $CaCl_2$. Solutions were prepared with HPLC grade water. Data were acquired with an Axopatch-1C amplifier and Axograph 4.5 software (Axon Instruments, Union City, CA). Unless noted, the membrane potential was clamped at –50 mV. Currents were filtered at 2 kHz and digitized at 5 kHz. Short -10 mV voltage steps before each agonist application were used to monitor cell input resistance (400-3000 MΩ). Drugs were applied by a fast microperfusion system. Unless noted, all solutions contained 100 μM glycine and agonist applications were made in 0 mM calcium. Percent block was calculated according the following equation: (1-(peak amplitude after MTS)/(peak amplitude before MTS)) X 100. The rate constant of MTSET modification was calculated from the equation derived by Wilson and Karlin (1998): (1/modification time constant) X (1/concentration of MTSET in M). Percent desensitization was calculated by the following equation: (1-(steady state current amplitude/peak current amplitude)) X 100. Data were expressed as mean ± SEM. ANOVA and Student's t test were used as appropriate with statistical significance set at $p < 0.05$.

Results

Screening accessibility in NR2A

Analysis of NR2A/NR2C chimeric mutant subunits indicates that the last four residues of the NR2A pre-M1 region, residues 553-556, influence glycine-independent desensitization (Krupp et al. 1998; Villarroel et al. 1998). We mutated residues in the pre-M1 and M1 domains to cysteines to examine their accessibility during channel gating (Figure 1A). The mutants were co-expressed in HEK293 cells with a C-terminal truncation mutant of NR1-1a (NR1-1a$_{stop838}$), which, unless noted, we will refer to as NR1. This NR1 truncation eliminates calcium-dependent inactivation thus simplifying analysis of desensitization (Figure 1A; Krupp et al. 1999). We examined the accessibility of each mutated residue using whole-cell recordings of NMDA receptor currents. Test pulses of glutamate and glycine were delivered before and after three 5-second applications of glycine with MTSET, or glutamate and glycine with MTSET (Figure 1B). MTSET had no effect on NR1/NR2A receptors in the absence of agonist, indicating that modification of endogenous cysteines does not alter channel gating. However MTSET caused a rapid, but completely reversible, inhibition of NR1/NR2A currents (not shown, but see Figure 1B, lower trace). This was attributable to open channel block by the charged MTSET rather than cysteine modification and thus did not interfere with analysis of the mutants.

Of the twelve residues we analyzed, cysteine-substitution altered the control responses of receptors containing NR2A$_{f549c}$, NR2A$_{l550c}$, NR2A$_{f553c}$, or NR2A$_{w558c}$ subunits. These currents were very small or had abnormal kinetics, and thus they were not further analyzed. Of the remaining eight residues, only a single residue, V557C, was

modified by MTSET during gating. As shown in Figure 1B, NR1/NR2A$_{v557c}$ currents showed irreversible block of NMDA receptor inward current following 3 applications of MTSET (48 ± 3.1%, n = 19). The fast decaying peak during MTSET applications was due to reversible block of open channels as also seen with NR1/NR2A channels. The tail current that immediately followed the end of each MTSET application represented unblock of open channels. NR1/NR2A$_{a548c}$ currents were irreversibly blocked by MTSET alone (78.4 ± 6.8%, n = 7, in the presence of glycine), indicating that the accessibility of A548C was not linked to channel gating. We subsequently focused our experiments on the modification of V557C during channel gating.

Substitution of MTSET with MTSEA, a smaller positively charged MTS reagent, or MTSHE, a smaller uncharged MTS reagent, only slightly increased the irreversible block of NR1/NR2A$_{v557c}$ currents (61.98 ± 3.9%, n = 7 & 56.76 ± 2.4%, n = 5), suggesting that the size and charge of MTSET did not impede accessibility (Karlin and Akabas 1998). To examine whether glutamate binding alone could alter the accessibility of V557C, we blocked the glycine-site on NR1 with 7-chlorokynurenic acid thus preventing channel activation (Figure 2). Under these conditions, glutamate application in the presence of MTSET did not cause a significant irreversible block of NR1/NR2A$_{v557c}$ currents (14.9 ± 4.2%, n = 10).

Modification rates of V557C and its homologous residue in NR1

We determined the MTSET modification rate of NR2A$_{v557c}$ by recording NR1/ NR2A$_{v557c}$ currents before and after single glutamate, glycine, and MTSET applications of increasing durations (5-60 seconds, Figure 3). Irreversible MTSET block increased

exponentially, reaching 88.3 ± 2.7% block after 60 seconds. The MTSET block was fit with a single exponential resulting in a time constant of 18.6 seconds that corresponds to a rate constant of 26.88 $s^{-1}M^{-1}$ (Wilson and Karlin 1998). A 15-second application of MTSET blocked a similar amount of current (53.86 ± 7.2%, n = 7) as three 5-second applications. Thus the accessibility of the V557C residue had reached equilibrium during the 5-second applications (Horn 1998).

Using SCAM analysis of the NR1 subunit expressed with a C-terminally truncated NR2C subunit containing an NR2A M1 domain ($NR2C^{M1}$), Beck et al. (1999) reported that $leucine^{562}$ ($leucine^{544}$ in their nomenclature) on NR1-1a was modified in the presence of glutamate and glycine (~ 67 %, 2 min, 3 mM MTSET). $Leucine^{562}$ on NR1-1a is homologous to $valine^{557}$ on NR2A. However MTSET did not irreversibly block $NR1\text{-}1a_{I562C}$/NR2A currents in the presence of glutamate and glycine using the protocol shown in Figure 1. As shown in Figure 3C, $NR1\text{-}1a_{I562C}$/NR2A currents were only modified after long applications of glutamate, glycine and MTSET (40 ± 3%, 2 min, 2 mM MTSET, n = 6). Thus the accessibility of L562C on NR1-1a was slower when expressed with NR2A subunits than with $NR2C^{M1}$ (Beck et al. 1999). Applications longer that 2 minutes can be damaging to cells, thus we did not attempt to determine a modification rate for the L562C mutant.

Desensitization and accessibility of V557C

Krupp et al. (1998) reported a series of modified NR2 constructs that demonstrate enhanced or reduced NMDA receptor desensitization. We introduced the V557C mutation into these constructs and tested for MTSET modification.

$NR2C_0A_{v557c}$ and $NR2D001/AD1_{v557c}$ are NR2C/NR2A chimeras in which all or most of the N-terminus sequence is from NR2C, whereas the rest of the sequence is taken from NR2A (Krupp et al. 1998). These subunits, when expressed with $NR1\text{-}1a_{stop838}$, did not desensitize and were not irreversibly blocked by MTSET (Figure 4). Conversely, the truncation mutant, $NR2A_{stop844v557c}$, which showed significant desensitization, had more irreversible block than full-length NR2A. These results suggested that there was a correlation between desensitization and V557C accessibility. However, $NR2AD1_{v557c}$, which has three mutations, F553Y, A555P and S556A, that convert the pre-M1 region to the NR2C sequence, appeared to behave anomalously. It desensitized, but was not irreversibly blocked by MTSET. This likely reflects modification of desensitization by domains other than pre-M1. Specifically, the binding of nanomolar zinc to the LIVBP-like domain (Zheng et al. 2001) likely accounts for macroscopic desensitization in $NR1/NR2AD1_{v557c}$ receptors. This is consistent with previous studies indicating that the LIVBP-like domain and the pre-M1 region contribute to glycine-independent desensitization (Krupp et al. 1998; Villarroel et al. 1998).

Modifying desensitization and accessibility

If V557C accessibility occurs only when the channel is desensitized, then preventing or enhancing desensitization should alter modification by MTSET. We took two approaches to address this prediction. Tetrapentylammonium (TPentA) and 9–aminoacridine (9-AA) block open NMDA channels (Benveniste and Mayer 1995; Costa and Albuquerque 1994; Sobolevsky 1999; Sobolevsky et al. 1999), and thus have been reported to block entry into desensitized states. We tested whether their presence

during channel gating might prevent MTSET modification of NR1/NR2A$_{v557c}$ receptors. Co-application of TPentA (1 mM) with MTSHE, glutamate, and glycine did not reduce irreversible block of NR1/NR2A$_{v557c}$ currents (47.7 ± 10.5%, n = 5). However TPentA only slightly prevented desensitization (36.1 ± 2.2% desensitization in control compared to 21.6 ± 4% desensitization in TPentA, n = 7). 9-aminoacridine (100 μM) reduced irreversible MTSET block in two cells (24% and 22%). However, the effect of 9-AA was overcome when we used 10 mM MTSET (66.3 ± 5.6%, n = 4). If one assumes that 9-AA prevents desensitization, then the result with 10 mM MTSET suggests that 9-AA and MTSET compete for binding within the pore or that 9-AA affects the accessibility of MTSET to V557C.

Another way to alter desensitization is by altering intracellular calcium. Influx of calcium through NMDA receptors increases desensitization as a result of calcineurin (CaN) activation (Krupp et al. 2002). Thus we tested if enhancing desensitization with calcium influx would increase the accessibility of V557C. Following 5-second applications of glutamate, glycine, and calcium (2 mM) to activate CaN, we measured MTSET modification of V557C in calcium-free solutions (Figure 5). Calcium influx increased the desensitization and the irreversible block of currents mediated by NR1/NR2A$_{v557c}$. Furthermore, calcium influx induced modification of NR1/NR2AD1$_{v557c}$ receptors. This protocol did not affect the accessibility of the homologous L562C residue in NR1. Calcium influx significantly increased desensitization of NR1-1a$_{l562c}$/NR2A but there was no detectable irreversible block (72.3 ± 3.7% desensitization, 8.8 ± 7.8% MTSET block, n = 4, data not shown).

The correlation between desensitization and the modification of V557C for the NR2A constructs is plotted in Figure 6 ($R = 0.86$, $p < 0.01$).

Discussion

Validity of method and comparison to prior results

The substituted-cysteine accessibility method has been used to infer conformational movements of several ion channels and ligand-gated receptors (Karlin and Akabas 1998). The general assumptions of the method are that cysteine substitution does not alter channel properties; that any changes in channel properties reflect modification of the substituted cysteine rather than native cysteines; and that the sufhydryl modification is irreversible. In many cases, these studies have been directed at the relatively constrained environment of the channel pore. Within the pore, the validity of the SCAM assumptions is relatively easy to establish. Changes in cysteine accessibility with channel activation have also been used to define residues involved in channel gating (Liu et al. 1996; Yang and Horn 1995). We applied this method to desensitization of NMDA receptors. Given the location of the pre-M1 region near the NMDA receptor extracellular vestibule and its importance in glycine-independent desensitization, we used SCAM to examine twelve residues in pre-M1 and the first transmembrane domain of NR2A. Four cysteine mutants yielded nonfunctional or abnormal currents when co-expressed with NR1-1a$_{stop838}$. The eight other cysteine mutants had normal current amplitudes and kinetics suggesting that cysteine substitution did not significantly alter their secondary structure. Although MTSET

blocked open NMDA channels, this effect was reversible and thus did not represent modification of native or substituted-cysteine residues.

SCAM has been used to define the structure of the pore and the extracellular vestibule of the NMDA receptor channel. In these studies, the number of modified residues in the pore was sensitive to the size of MTS reagents (Kuner et al. 1996). This indicated that the pore is a narrow structure formed by M2 domains centered on the magnesium-binding site. M3 domains occupy most of the extracellular vestibule whereas portions of pre-M1, M1, and M4 contribute to the vestibule. MTS reagents modify many residues in the vestibule in the absence of channel activation (Beck et al. 1999). In our experiments, MTSET irreversibly blocked currents mediated by receptors containing $NR2A_{a548c}$ or $NR2A_{v557c}$, but only modification of $NR2A_{v557c}$ required channel gating. Both glutamate and the co-agonist glycine were required for modification of V557C, suggesting that the change in accessibility involved a concerted action of NR1 and NR2 subunits, rather than a direct effect of glutamate binding to the NR2 subunit.

The changes in accessibility of V557C with gating are unique within the preM1-M1 region. Previous studies reported that the homologous residue in NR1 also is modified by MTSET (Beck et al. 1999). In those experiments $NR1\text{-}1a_{l562c}$ (L544 in the terminology of Beck et al.) was expressed with a modified NR2C subunit in *Xenopus* oocytes. When we expressed the same construct with wild-type NR2A, the modification was less. This result suggests that NR2 subunits influence L562C accessibility on NR1. The different rates of accessibility for V557C on NR2 and L562C on NR1 may also

reflect asymmetrical gating of NR1 and NR2 subunits (Wollmuth and Sobolevsky 2004).

Channel blockers and NMDA channel gating

Using channel blockers of varying sizes, Sobolevsky et al. (1999) reported that small blockers, such as tetraethylammonium (TEA), were trapped in the open channel without affecting channel closure or desensitization, whereas a large blocker, tetrapentylammonium (TPentA), prohibited channel closure as well as desensitization. On this basis they proposed a physical model of NMDA receptor channel gating that contains distinct activation and desensitization "gates" with the activation gate placed closer to the extracellular surface. This idea was based on the fact that the intermediate size blocker, tetrabutylammonium (TBA), prevented channel closure, but not desensitization. However, placement of the activation gate near the extracellular surface is incompatible with the fact that many residues in the vestibule are accessible to MTS reagents in the absence of agonist (Beck et al. 1999). The SCAM analysis of non-desensitizing NR1/NR2C receptors suggests that the activation gate is deep within the pore formed by M3 segments whereas the pre-M1 and M4 segments form the more superficial lining of the extracellular vestibule. In this model, channel closure involves constriction of the deep part of the vestibule, thus trapping certain channel blockers (Sobolevsky et al. 2002).

This revised model leaves open the possibility that residues involved in desensitization might be located in the superficial parts of the vestibule. We expected that channel blockers that purportedly block desensitization would be useful to examine

changes in the accessibility of residues in the pre-M1/M1 region. Unfortunately, TPentA did not completely block desensitization in our experiments, and the effects of 9-aminoacridine were not interpretable due to its competition with MTSET, itself an NMDA channel blocker. Thus the use of channel blockers was not sufficient in our hands to define the domains involved in NMDA receptor desensitization.

Modification of V557C and desensitization

Different combinations of NMDA receptor subunits have striking differences in desensitization. The amino acid sequence differences between desensitizing NR2A subunits and nondesensitizing NR2C subunits were used to show that the pre-M1 region and the LIVBP-like domain in the N-terminus are involved in NMDA receptor desensitization (Krupp et al. 1998; Villarroel et al. 1998). Our results provide further evidence that residues in the pre-M1 region are sensitive to gating steps associated with desensitization. The overall correlation between desensitization and MTSET modification suggests that V557C, the first residue in M1, was only modified when the receptor was in the desensitized state. This correlation was supported by the increases in MTSET modification resulting from calcium-induced increases in desensitization of NR1/NR2A$_{v557c}$ currents. These last results also support the idea that intracellular regulation of NR2A modifies desensitization at a distance by affecting regions at, or surrounding, V557C. This action of the intracellular domain of NR2A, possibly influenced by an intracellular protein-protein interaction, could alter the confirmation of the N-terminal domain (Krupp et al. 2002).

In addition to the pre-M1 region, the LIVBP-like domain also influences desensitization. The effect of the LIVBP-like domain may explain the apparently anomalous behavior of the NR2AD1$_{v557c}$ mutant that is identical to NR2A except for an NR2C pre-M1 region. This mutant showed desensitization, likely due to a modulatory effect of zinc (Zheng et al. 2001), as discussed earlier. However, when desensitization in this mutant was enhanced by CaN activation, the receptor was modified by MTSET. Thus accessibility of V557C is a reliable detector of desensitization.

A structural view of desensitization gating

Our results indicate that modification of V557C correlates with NMDA receptor desensitization. The proximity of valine^{557} to the pre-M1 region fits with a critical role of that region in desensitization, but, as discussed above, the LIVBP-like domain and regulatory effects in the C-terminus also contribute. Models based primarily on studies of the channel pore cannot account for these more distant effects (Sobolevsky et al. 1999), nor can they account for the coupling between ligand binding and channel gating. Thus, it is necessary to incorporate a model of conformational changes associated with ligand binding to understand desensitization. Such information largely comes from studies of AMPA receptors.

The crystal structures of the ligand-binding pocket of AMPA receptors provide a framework to consider how ligand binding leads to channel gating including desensitization. Structures with and without ligands have provided information on the conformational movements triggered by ligand binding, that have been tested in functional studies (Mayer and Armstrong 2004; Sun et al. 2002). These studies indicate

that movements in ligand-binding domains directly cause changes in gating. Several basic features emerge that are likely shared among ionotropic glutamate receptors. Each AMPA receptor is a tetramer comprised of two subunit pairs. The subunits within each pair non-covalently interact with each other through their S1 domains. Glutamate initially binds to the S1 pocket of an open S1-S2 clamshell causing displacement of S2 away from the plasma membrane as it closes around the ligand. This S2 movement causes channel gating by pulling the M3 domains up and away from each other. The open channel confirmation puts tension on the interactions between a pair of S1 domains. Desensitization occurs when S1-S1 interactions rearrange into a more stable confirmation causing transmembrane domains to relax and close the channel (Horning and Mayer 2004).

Although there is less structural information on NMDA receptor subunits, there are reasons to expect similarities with AMPA receptors. NMDA and AMPA receptors share similar kinetic schemes; they have very similar secondary structures; the crystal structure of the NR1 ligand-binding domain is similar to AMPA subunits; NR2A requires a portion of the LIVBP-like domain near the S1 of NR1 for surface expression; and the region around the LIVBP/S1 border mediates negative cooperativity between NR1 and NR2 subunits (Furukawa and Gouaux 2003; Inanobe et al. 2005; Meddows et al. 2001; Regalado et al. 2001; Wollmuth and Sobolevsky 2004). Assuming that NMDA receptors are NR1/NR2 dimers of dimers arranged in 1-1-2-2 tetramers, (Schorge and Colquhoun 2003), desensitization may involve a relaxation in S1-S1 interfaces. Our results suggest that this relaxation is sensed by the linker connecting S1 to M1, resulting in the accessibility of V557C in NR2A (the glutamate binding subunit). Interestingly,

the homologous NR1 residue was actually more accessible in a non-desensitizing receptor (Beck et al. 1999). The change in accessibility of V557C is consistent with a specific role of the pre-M1 region in NMDA receptor desensitization. Our data cannot resolve whether the putative relaxation of the S1-S1 interface simply reveals V557C, making it a sensitive detector of the desensitized state, or if V557C is the desensitization "gate". Even if the latter is true, our data confirm that the LIVBP-like domain can independently influence desensitization and thus presumably the S1-S1 relaxation. The modulation by CaN further suggests that intracellular domains can induce conformational changes in ligand-binding domains.

Acknowledgements

This work was supported by National Institutes of Health Grants MH46613 (G.L.W.) and NS28709 (S.F.H.); Biofirst Award, NSW (B.V.); NHMRC188819 (B.V.); C.J. Martin Fellowship, NHMRC (EEB). We thank Dr. Lonnie P. Wollmuth for the NR1-1a$_{I562c}$ clone. We also thank Ashleigh J. Miller for preparing cDNAs and HEK293s.

Figure Legends

Figure 1. MTSET modification of NR2A$_{V557c}$ occurred in a state-dependent manner. A: Diagram of the NR2A subunit. Residues around the pre-M1/M1 border (enlarged) were individually mutated to cysteine (bold lettering). Valine^{557} is underlined. B: MTSET modification screening protocols. Top and bottom recordings are from two different HEK293 cells expressing the NR1-1a$_{stop838}$/NR2A$_{V557c}$ subunit combination. Test pulses

of glutamate (1 mM) and glycine (100 μM) were recorded before (extreme left) and after (extreme right) three applications of glutamate, glycine, and MTSET (2 mM, top traces) or glycine and MTSET (bottom traces). The test pulses are averages of 3-4 responses. C: The irreversible block by MTSET was plotted for each cysteine-substituted NR2A subunit using the protocol in panel B. Data represents mean ± SEM (* = significant compared to wild type NR2A; ANOVA with Bonferroni/Dunn post-hoc test $p < 0.0005$; ** = significantly different than % block for V557C tested with glycine and MTSET, unpaired *t*-test $p < 0.0001$).

Figure 2. MTSET modification of $NR2A_{v557c}$ requires channel gating. Currents mediated by NR1-$1a_{stop838}$/$NR2A_{v557c}$ receptors were recorded in the presence of glutamate and glycine immediately before and after three applications of glutamate (1 mM), 7-chlorokynurenic acid (100 μM, 7CKA), and MTSET (2 mM). The glycine antagonist, 7CKA, completely blocked the evoked current as well as glutamate- and glycine-dependent modification by MTSET. The irreversible block after three applications of 7CKA and MTSET (8.8 ± 2.7%, n = 6; unpaired *t*-test) was the same as for glutamate, 7CKA and MTSET (14.9 ± 4.2%, n = 10). The small reduction was caused by gradual rundown of current amplitudes.

Figure 3. MTSET modification rates for $NR2A_{v557c}$ and NR1-$1a_{l562c}$. A: Example responses from cells transfected with NR1-$1a_{stop838}$/$NR2A_{v557c}$ (top) and NR1-$1a_{l562c}$/NR2A (bottom). Test pulses were recorded before (left-hand traces) and after (right-hand traces) a 60-second application of glutamate, glycine, and MTSET (middle

traces). Test pulses are averages of 3-4 traces. B: MTSET modification rates for each clone, derived from the % irreversible block observed after different MTSET application lengths. Each point is the average of at least 6 cells. The NR1-1$a_{stop838}$/NR2A$_{v557c}$ averages were fit with a single exponential. MTSET block of NR1-1$a_{stop838}$/NR2A$_{v557c}$ responses recorded after 30, 45, and 60-second applications of glutamate, glycine, MTSET were not significantly different from each other (ANOVA and a Bonferroni/Dunn post-hoc test). For NR1-1a_{l562c}/NR2A responses, only a 120-second application of glutamate, glycine, and MTSET caused significant block ($p < 0.0001$).

Figure 4. MTSET modification of NR2A$_{v557c}$ correlates with increased desensitization. A, left-hand column: Diagram of V557C clones. Black bars represent NR2C sequence and white bars represent NR2A sequence. Middle and left-hand columns are representative test pulse responses from each construct, expressed with NR1-1$a_{stop838}$, recorded before (middle column) and after (right-hand column) three, 5-second applications of glutamate, glycine, and MTSET. B: Summary of average % desensitization and % MTSET block. ANOVA with a Bonferroni/Dunn post-hoc test was used to analyze differences (NR2C0A$_{v557c}$, n = 3; NR2D001/AD1$_{v557c}$, n = 7; NR2AD1$_{v557c}$, n = 5; NR2A$_{v557c}$, n = 19; NR2A$_{stop844v557v}$, n = 7; * = significantly different than NR2A$_{v557c}$, $p < 0.0001$ for % desensitization; $p < 0.0005$ for % block).

Figure 5. Calcium influx increases desensitization and MTSET block in NR2A$_{v557c}$- and NR2AD1$_{v557c}$- containing receptors. A: Examples of recordings from NR1-

$1a_{stop838}$/$NR2A_{v557c}$- and NR1-$1a_{stop838}$/$NR2AD1_{v557c}$- transfected cells (top and bottom traces, respectively). Initial glutamate and glycine test pulses (left) show very little desensitization. Subsequent glutamate and glycine applications in the presence of calcium (2 mM, middle traces) decreased the current amplitude and increased desensitization. Test pulses recorded again in calcium-free conditions before and after applying glutamate, glycine, and MTSET three times (right-hand traces). B: Average % desensitization and average % MTSET block measured after calcium treatment (Ca^{2+}Tx) of each clone. Unpaired *t*-tests were used to compare $NR2A_{v557c}$ with $NR2A_{v557c}$ after Ca^{2+}Tx averages (*, $p < 0.0001$ for % block) and $NR2AD1_{v557c}$ with $NR2AD1_{v557c}$ after Ca^{2+}Tx averages (**, $p < 0.02$ for % block and $p < 0.01$ for % desensitization).

Figure 6. MTSET modification correlates with desensitization. Data from Figures 4 and 5 were combined and plotted as a correlation. A line fit of the data yields a correlation coefficient of 0.86, $p < 0.01$.

Figure 1

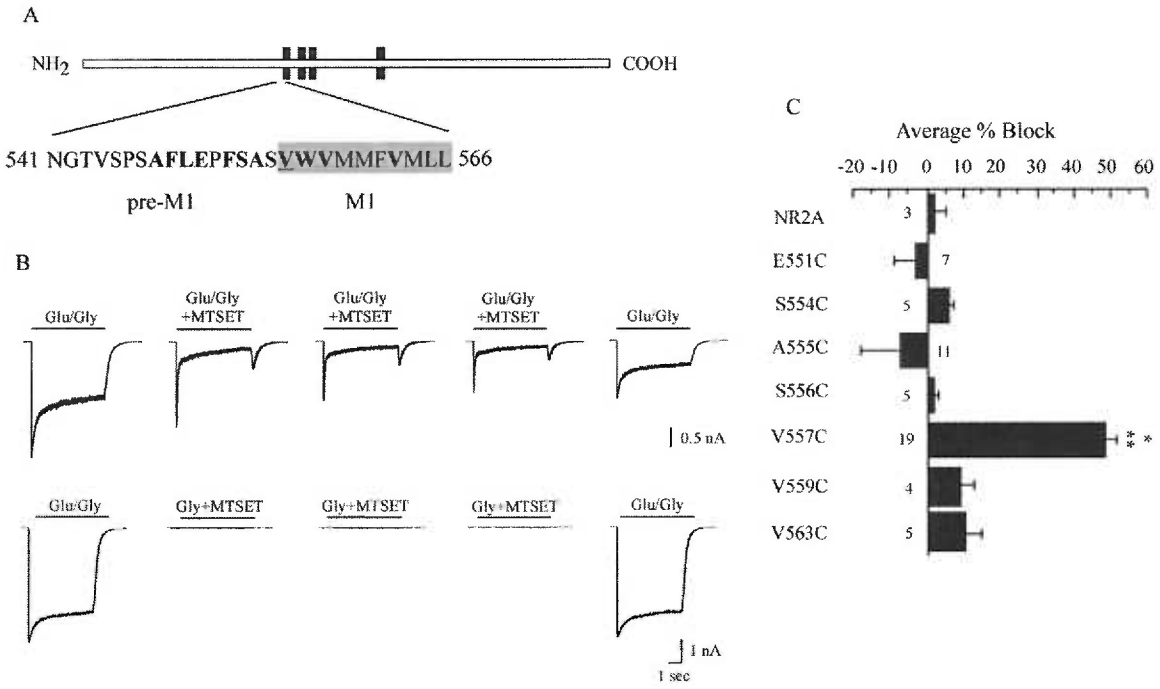
A
NH2
COOH
541 NGTVSPSAFLEPFSASVWVMMFVMLL 566
pre-M1
M1
B
Glu/Gly
Glu/Gly +MTSET
Glu/Gly +MTSET
Glu/Gly +MTSET
Glu/Gly
0.5 nA
Glu/Gly
Gly+MTSET
Gly+MTSET
Gly+MTSET
Glu/Gly
1 nA
1 sec
C
Average % Block
-20 -10 0 10 20 30 40 50 60
NR2A 3
E551C 7
S554C 5
A555C 11
S556C 5
V557C 19 ** *
V559C 4
V563C 5

Figure 2

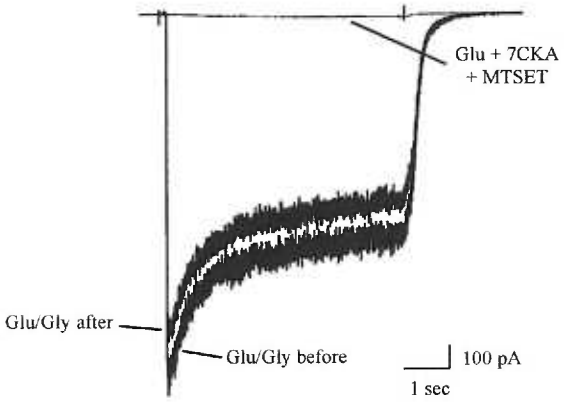

Figure 3

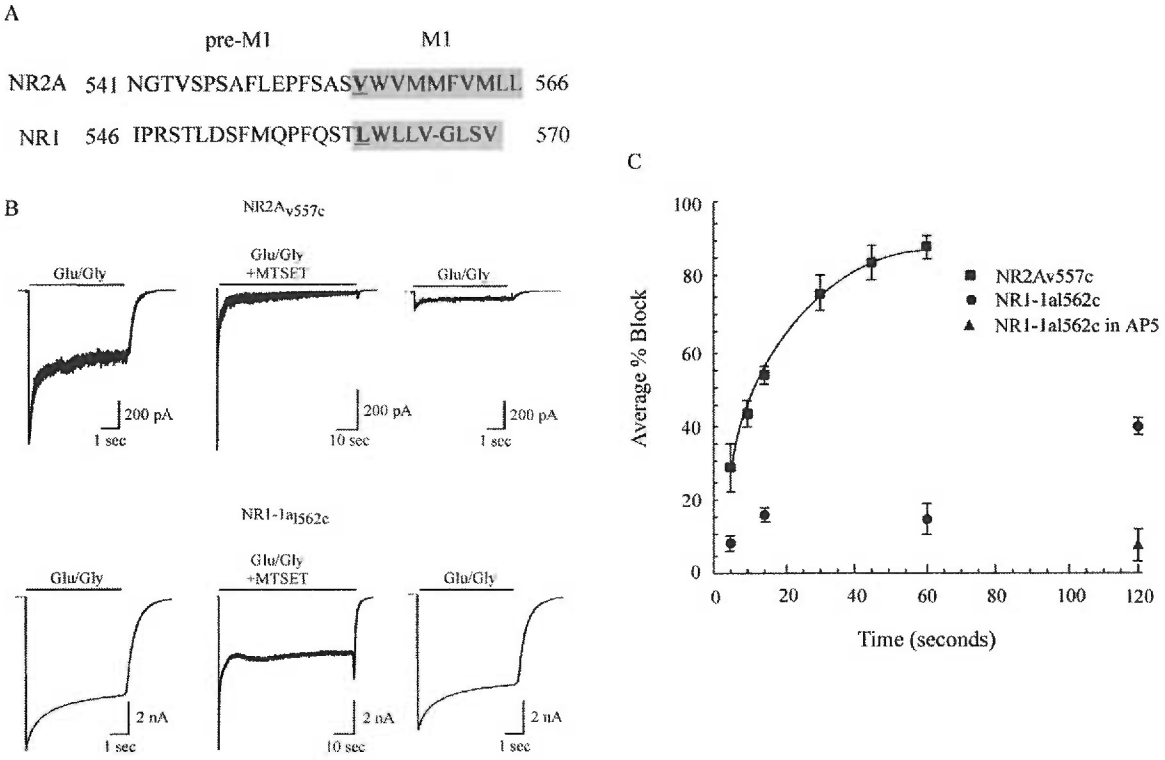
A
pre-M1
M1
NR2A 541 NGTVSPSAFLEPFSASVWVMMFVMLL 566
NR1 546 IPRSTLDSFMQPFQSTLWLLV-GLSV 570
B
NR2Av557c
Glu/Gly
Glu/Gly +MTSET
Glu/Gly
200 pA
1 sec
200 pA
10 sec
200 pA
1 sec
NR1-1a1562c
Glu/Gly
Glu/Gly +MTSET
Glu/Gly
2 nA
1 sec
2 nA
10 sec
2 nA
1 sec
C
Average % Block
Time (seconds)
NR2Av557c
NR1-1a1562c
NR1-1a1562c in AP5

Figure 4

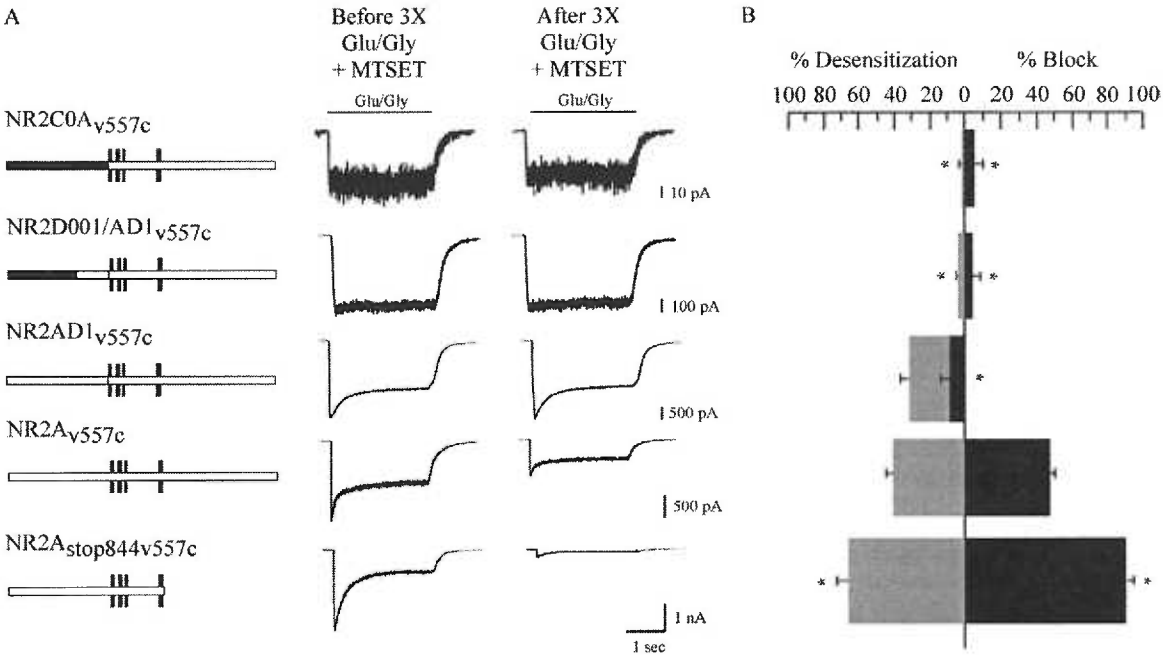
A
Before 3X
Glu/Gly
+ MTSET
After 3X
Glu/Gly
+ MTSET
Glu/Gly
Glu/Gly
NR2C0A v557c
NR2D001/AD1 v557c
NR2AD1 v557c
NR2A v557c
NR2A stop844v557c
10 pA
100 pA
500 pA
500 pA
1 nA
1 sec
B
% Desensitization
% Block
100 80 60 40 20 0 20 40 60 80 100

Figure 5

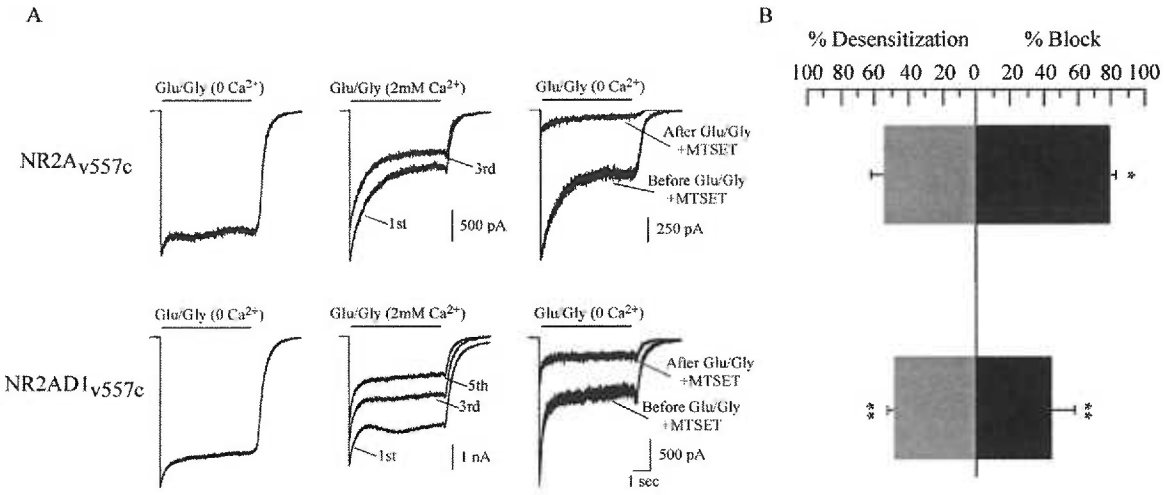
A
Glu/Gly (0 Ca2+)
Glu/Gly (2mM Ca2+)
Glu/Gly (0 Ca2+)
NR2Av557c
3rd
1st
500 pA
After Glu/Gly +MTSET
Before Glu/Gly +MTSET
250 pA
NR2AD1v557c
5th
3rd
1st
1 nA
500 pA
1 sec
B
% Desensitization
% Block
100 80 60 40 20 0 20 40 60 80 100
*
**
**

Figure 6

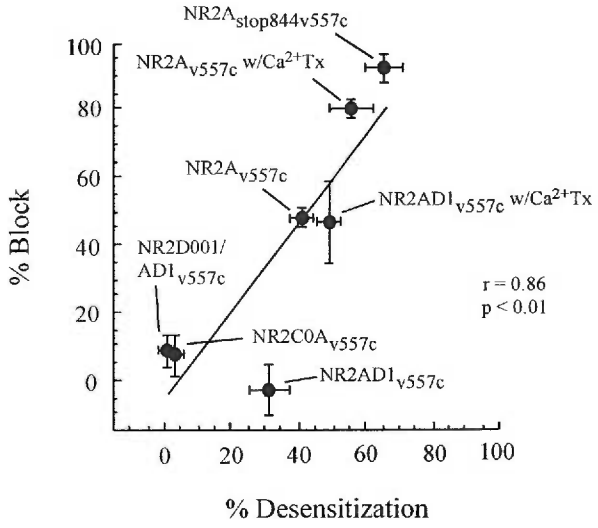
NR2A stop844v557c
NR2A v557c w/Ca2+Tx
NR2A v557c
NR2AD1 v557c w/Ca2+Tx
NR2D001/
AD1 v557c
NR2C0A v557c
NR2AD1 v557c
r = 0.86
p < 0.01
% Block
% Desensitization
0
20
40
60
80
100

Summary

My thesis research examined how NMDA receptor subunits influence the modulation, targeting, and gating of NMDA receptors. Each of these issues is important because they influence postsynaptic signaling.

Modulation

I contributed to two studies that are not included as chapters in the thesis. In the first, we reported that Ca^{2+}-dependent inactivation was dependent on the C0 cassette of the NR1 intracellular domain (Krupp et al. 1999). The intracellular proteins, Ca^{2+}/calmodulin and α-actinin competitively bind to C0 and subsequently modulate inactivation. Binding of α-actinin inhibited inactivation whereas Ca^{2+}/calmodulin binding induced inactivation. In the second study, we showed that two amino acid residues on NR2A, serines 900 and 929, modulated glycine-independent desensitization by calcineurin (Krupp et al. 2002). Our results suggest that residue 900 is the residue dephosphorylated by calcineurin, resulting in enhanced desensitization. Dephosphorylation of 929 prevents calcineurin from interacting with the NR2A subunit.

Targeting

As shown in Figure 1D of Chapter 1, NR2 subunits significantly influence NMDA receptor responses. We reexamined the subunit composition of synaptic and extrasynaptic NMDA receptors because both have been implicated in postsynaptic signaling. Our results showed that NR2A and NR2B subunits were present in both synaptic and extrasynaptic receptors. NR2 subunit distribution can vary depending on

the tissue preparation. Thus our results support the idea that NR2A and NR2B subunits contribute to synaptic and extrasynaptic receptors. Further experiments showed that NR2A subunits lacking the C-terminal, intracellular domain were also present in both synaptic and extrasynaptic receptors. Thus protein interactions or modulation involving the loss of the C-terminal, intracellular domain was not absolutely required for NR2A distribution. However truncation significantly reduced NR2A incorporation into synaptic and extrasynaptic receptors suggesting that truncation disrupted the processing, i.e. assembly, trafficking, or degradation, of NR2A-containing receptors.

Future Directions

The results presented in Chapter 1 raise at least two issues for future studies. One issue is where NMDA receptors insert. It has been hypothesized that extrasynaptic NMDA receptors serve as a reserve pool for synaptic receptors (Perez-Otano and Ehlers 2004). If true, then one expects that newly inserted receptors should first appear at extrasynaptic locations. Using whole-cell recordings from cultured hippocampal neurons, Lan et al. (2001) and Mu et al. (2003) showed that activation of PKC and treatment with TTX increased the recovery of whole-cell NMDA receptor currents after blocking them with whole-cell applications of NMDA and MK-801. Assuming that activation of PKC or treatment with TTX does not affect MK-801 binding, their results suggest that these treatments increase the insertion of new NMDA receptors. A similar protocol could be used in autaptic cultures to determine whether newly inserted NMDA receptors appear in synaptic or extrasynaptic sites.

A second issue is what regions of the NR2A C-terminus are needed for surface expression. For instance, is incorporation dependent on the PDZ domain as Barria et al. (2002) reported? The Westbrook lab has NR2A C-terminal truncation mutants that vary in length. Measurement of the ifenprodil inhibition from $NR2A^{-/-}$ neurons transfected with the different truncation mutants could help narrow down the region that is necessary for full incorporation.

Gating

We used the substituted-cysteine accessibility method (SCAM) to determine whether the accessibility of residues in the pre-M1 region and M1 domain changed during desensitization. Our results showed that the V557C residue was the only residue modified during gating, that it required glutamate and glycine binding, and that its accessibility correlated with desensitization. We concluded that, with the exception of the $NR2AD1_{v557c}$ mutant, the V557C residue detected desensitization. However it was not clear whether V557C detected desensitization because it is part of a desensitization gate or rather detected conformational changes in the receptor associated with desensitization, e.g. S1-S1 interactions.

Future Directions

Experiments on $NR1/NR2AD1_{v557c}$ receptors showed that the V557C residue was not accessible even though the currents desensitized. The NR2AD1 subunit is an NR2A subunit with an NR2C pre-M1 region. As Zheng et al. (2001) have shown, desensitization of these receptors may be due to voltage-independent zinc inhibition,

which is modulated by the LIVBP-like domain in the extreme N-terminus of NR2A. Thus it would be interesting to determine whether NR1/NR2AD1 desensitization is due to zinc, e.g. by chelating it with TPEN. If so, then it may also be interesting to determine whether zinc chelation affects the accessibility of V557C in NR1/NR2A$_{v557c}$ receptors. Similarly, a V557C mutant of D001 (D001$_{v557c}$), an NR2A subunit that has an NR2C LIVBP-like domain (Krupp et al. 1998), should provide the equivalent situation as chelating zinc during NR1/NR2A$_{v557c}$ recordings. According to the results presented in Chapter 2, neither zinc chelation of NR1/NR2A$_{v557c}$ receptors nor the presence of an NR2C LIVBP-like domain in NR1/D001$_{v557c}$ receptors should affect MTSET modification of V557C.

The lurcher motif, SYTANLAAF, of NR1 and NR2 subunits has been implicated in the coupling of ligand binding to channel gating (Kohda et al. 2000), and is thus another region that could be examined for accessibility changes during desensitization by using SCAM. Jones et al. (2002), showed that cysteine-substitution of the second alanine in the lurcher motif (SYTANLCAF) was modified in a state-dependent manner, similar to our results with V557C. These results suggest we could make a similar mutation in NR2 subunits with varying desensitization properties to investigate whether desensitization affects movement in the lurcher motif of NR2A.

Finally, by combining electrophysiological techniques with X-crystallography, Sun et al. (2002) provide a compelling model for AMPA receptor gating. A similar structural approach may be required to understand the conformational changes associated with NMDA receptor gating.

References

Amparan D, Avram D, Thomas CG, Lindahl MG, Yang J, Bajaj G, and Ishmael JE. Direct interaction of myosin regulatory light chain with the NMDA receptor. *Journal of Neurochemistry* 92: 349-361, 2005.

Barlowe C. Signals for COPII-dependent export from the ER: what's the ticket out? *Trends in Cell Biology* 13: 295-300, 2003.

Barria A and Malinow R. Subunit-specific NMDA receptor trafficking to synapses. *Neuron* 35: 345-353, 2002.

Beck C, Wollmuth LP, Seeburg PH, Sakmann B, and Kuner T. NMDAR channel segments forming the extracellular vestibule inferred from the accessibility of substituted cysteines. *Neuron* 22: 559-570, 1999.

Bekkers JM and Stevens CF. Excitatory and inhibitory autaptic currents in isolated hippocampal neurons maintained in cell culture. *Proc Natl Acad Sci U S A* 88: 7834-7838, 1991.

Benveniste M and Mayer ML. Trapping of glutamate and glycine during open channel block of rat hippocampal neuron NMDA receptors by 9-aminoacridine. *Journal of Physiology* 483: 367-384, 1995.

Blanpied TA, Scott DB, and Ehlers MD. Dynamics and regulation of clathrin coats at specialized endocytic zones of dendrites and spines. *Neuron* 36: 435-449, 2002.

Bolton MM, Blanpied TA, and Ehlers MD. Localization and stabilization of ionotropic glutamate receptors at synapses. *Cell Mol Life Sci* 57: 1517-1525, 2000.

Chatterton JE, Awobuluyi M, Premkumar LS, Takahashi H, Talantova M, Shin Y, Cui J, Tu S, Sevarino KA, Nakanishi N, Tong G, Lipton SA, and Zhang D. Excitatory glycine receptors containing the NR3 family of NMDA receptor subunits. *Nature* 415: 793-798, 2002.

Chavis P and Westbrook G. Integrins mediate functional pre- and postsynaptic maturation at a hippocampal synapse. *Nature* 411: 317-321, 2001.

Chen N, Li B, Murphy TH, and Raymond LA. Site within N-Methyl-D-aspartate receptor pore modulates channel gating. *Molecular Pharmacology* 65: 157-164, 2004.

Chen N, Luo T, and Raymond LA. Subtype-dependence of NMDA receptor channel open probability. *Journal of Neuroscience* 19: 6844-6854, 1999.

Chen PE, Geballe MT, P.J. S, Johnston AR, Yuan H, Jacob AL, Snyder JP, Traynelis SF, and Wyllie DJ. Structural features of the glutamate binding site in Recombinant NR1/NR2A N-Methyl-D-aspartate receptors determined by site-directed mutagenesis and molecular modeling. *Molecular Pharmacology* 67, No. 5, 2005.

Clements JD and Westbrook GL. Activation kinetics reveal the number of glutamate and glycine binding sites on the N-methyl-D-aspartate receptor. *Neuron* 7: 605-613, 1991.

Colquhoun D and Hawkes AG. Desensitization of N-methyl-D-aspartate receptors: a problem of interpretation. *Proceedings of the National Academy of Sciences of the United States of America* 92: 10327-10329, 1995.

Costa AC and Albuquerque EX. Dynamics of the actions of tetrahydro-9-aminoacridine and 9-aminoacridine on glutamatergic currents: concentration-jump

studies in cultured rat hippocampal neurons. *Journal of Pharmacology & Experimental Therapeutics* 268: 503-514, 1994.

Cottrell JR, Dube GR, Egles C, and Liu G. Distribution, density, and clustering of functional glutamate receptors before and after synaptogenesis in hippocampal neurons. *J Neurophysiol* 84: 1573-1587, 2000.

Edmonds B, Gibb AJ, and Colquhoun D. Mechanisms of activation of glutamate receptors and the time course of excitatory synaptic currents. *Annual Review of Physiology* 57: 495-519, 1995.

Ehlers MD, Zhang S, Bernhadt JP, and Huganir RL. Inactivation of NMDA receptors by direct interaction of calmodulin with the NR1 subunit. *Cell* 84: 745-755, 1996.

Erreger K, Dravid SM, Banke TG, Wyllie DJ, and Traynelis SF. Subunit-specific gating controls rat NR1/NR2A and NR1/NR2B NMDA channel kinetics and synaptic signalling profiles. *J Physiol* 563.2, 2005.

Flint AC, Maisch US, Weishaupt JH, Kriegstein AR, and Monyer H. NR2A subunit expression shortens NMDA receptor synaptic currents in developing neocortex. *J Neurosci* 17: 2469-2476, 1997.

Furukawa H and Gouaux E. Mechanisms of activation, inhibition and specificity: crystal structures of the NMDA receptor NR1 ligand-binding core. *EMBO Journal* 22: 2873-2885, 2003.

Gottmann K, Mehrle A, Gisselmann G, and Hatt H. Presynaptic control of subunit composition of NMDA receptors mediating synaptic plasticity. *J Neurosci* 17: 2766-2774, 1997.

Groc L, Heine M, Cognet L, Brickley K, Stephenson FA, Lounis B, and Choquet D. Differential activity-dependent regulation of the lateral mobilities of AMPA and NMDA receptors. *Nature Neuroscience* 7: 695-696, 2004.

Guillaud L, Setou M, and Hirokawa N. KIF17 dynamics and regulation of NR2B trafficking in hippocampal neurons. *J Neurosci* 23: 131-140, 2003.

Hardingham GE, Fukunaga Y, and Bading H. Extrasynaptic NMDARs oppose synaptic NMDARs by triggering CREB shut-off and cell death pathways. *Nature Neuroscience* 5: 405-414, 2002.

Hatton CJ and Paoletti P. Modulation of triheteromeric NMDA receptors by N-terminal domain ligands. *Neuron* 46: 261-274, 2005.

Herin GA. Amino terminal domain regulation of NMDA receptor function. *European Journal of Pharmacology* 500, 2004.

Hoffmann H, Gremme T, Hatt H, and Gottmann K. Synaptic activity-dependent developmental regulation of NMDA receptor subunit expression in cultured neocortical neurons. *J Neurochem* 75: 1590-1599, 2000.

Hollmann M, Boulter J, Maron C, Beasley L, Sullivan J, Pecht G, and Heinemann S. Zinc potentiates agonist-induced currents at certain splice variants of the NMDA receptor. *Neuron* 10: 943-954, 1993.

Horn R. Explorations of voltage-dependent conformational changes using cysteine scanning. *Methods in Enzymology* 293: 145-155, 1998.

Horning MS and Mayer ML. Regulation of AMPA receptor gating by ligand binding core dimers. *Neuron* 41: 379-388, 2004.

Horten RM, Hunt HD, Ho SN, Pullen JK, and Pease LR. Engineering hybrid genes without the use of restriction enzyme: gene splicing by overlap extension. *Gene* 77: 61-68, 1989.

Hsu SC, Hazuka CD, Foletti DL, and Scheller RH. Targeting vesicles to specific sites on the plasma membrane: the role of the sec6/8 complex. *Trends in Cell Biology* 9: 150-153, 1999.

Inanobe A, Furukawa H, and Gouaux E. Mecahnism of Partial Agonist Action at the NR1 Subunit of NMDA Receptors. *Neuron* 47: 71-84, 2005.

Ishii T, Moriyoshi K, Sugihara H, Sakurada K, Kadotani H, Yokoi M, Akazawa C, Shigemoto R, Mizuno N, and Masu M. Molecular characterization of the family of the N-methyl-D-aspartate receptor subunits. *Journal of Biological Chemistry* 268: 2836-2843, 1993.

Ito I, Kawakami R, Sakimura K, Mishina M, and Sugiyama H. Input-specific targeting of NMDA receptor subtypes at mouse hippocampal CA3 pyramidal neuron synapses. *Neuropharmacology* 39: 943-951, 2000.

Jahr CE and Stevens CF. Glutamate activates multiple single channel conductances in hippocampal neurons. *Nature* 325: 522-525, 1987.

Jones KS, VanDongen HM, and VanDongen AM. The NMDA receptor M3 segment is a conserved transduction element coupling ligand binding to channel opening. *Journal of Neuroscience* 22: 2044-2053, 2002.

Jones MV and Westbrook GL. The impact of receptor desensitization on fast synaptic transmission. *Trends in Neurosciences* 19: 96-101, 1996.

Karlin A and Akabas MH. Substituted-cysteine accessibility method. *Methods in Enzymology* 293: 123-145, 1998.

Kew JN, Richards JG, Mutel V, and Kemp JA. Developmental changes in NMDA receptor glycine affinity and ifenprodil sensitivity reveal three distinct populations of NMDA receptors in individual rat cortical neurons. *J Neurosci* 18: 1935-1943, 1998.

Kim E, Cho KO, Rothschild A, and Sheng M. Heteromultimerization and NMDA receptor-clustering activity of Chapsyn-110, a member of the PSD-95 family of proteins. *Neuron* 17: 103-113, 1996.

Kim E and Sheng M. PDZ domain proteins of synapses. *Nature Reviews Neuroscience* 5: 771-781, 2004.

Kirson ED and Yaari Y. Synaptic NMDA receptors in developing mouse hippocampal neurones: functional properties and sensitivity to ifenprodil. *J Physiol* 497 (Pt 2): 437-455, 1996.

Kohda K, Wang Y, and Yuzaki M. Mutation of a glutamate receptor motif reveals its role in gating and delta2 receptor channel properties. *Nature Neuroscience* 3: 315-322, 2000.

Krupp JJ, Vissel B, Heinemann SF, and Westbrook GL. Calcium-dependent inactivation of recombinant N-methyl-D-aspartate receptors is NR2 subunit specific. *Molecular Pharmacology* 50: 1680-1688, 1996.

Krupp JJ, Vissel B, Heinemann SF, and Westbrook GL. N-terminal domains in the NR2 subunit control desensitization of NMDA receptors. *Neuron* 20: 317-327, 1998.

Krupp JJ, Vissel B, Thomas CG, Heinemann SF, and Westbrook GL. Calcineurin acts via the C-terminus of NR2A to modulate desensitization of NMDA receptors. *Neuropharmacology* 42: 593-602, 2002.

Krupp JJ, Vissel B, Thomas CG, Heinemann SF, and Westbrook GL. Interactions of calmodulin and alpha-actinin with the NR1 subunit modulate Ca^{2+}-dependent inactivation of NMDA receptors. *Journal of Neuroscience* 19: 1165-1178, 1999.

Kuner T, Seeburg PH, and Guy HR. A common architecture for K^+ channels and ionotropic glutamate receptors? *Trends in Neurosciences* 26: 27-32, 2003.

Kuner T, Wollmuth LP, Karlin A, Seeburg PH, and Sakmann B. Structure of the NMDA receptor channel M2 segment inferred from the accessibility of substituted cysteines. *Neuron* 17: 343-352, 1996.

Kutsuwada T, Kashiwabuchi N, Mori H, Sakimura K, Kushiya E, Araki K, Meguro H, Masaki H, Kumanishi T, and Arakawa M. Molecular diversity of the NMDA receptor channel. *Nature* 358: 36-41, 1992.

Lan JY, Skeberdis VA, Jover T, Grooms SY, Lin Y, Araneda RC, Zheng X, Bennett MV, and Zukin RS. Protein kinase C modulates NMDA receptor trafficking and gating. *Nature Neuroscience* 4: 382-390, 2001.

Laube B, Schemm R, and Betz H. Molecular determinants of ligand discrimination in the glutamate-binding pocket of the NMDA receptor. *Neuropharmacology* 47: 994-1007, 2004.

Lavezzari G, McCallum J, Dewey CM, and Roche KW. Subunit-specific regulation of NMDA receptor endocytosis. *Journal of Neuroscience* 24: 6383-6391, 2004.

Lavezzari G, McCallum J, Lee R, and Roche KW. Differential binding of the AP-2 adaptor complex and PSD-95 to the C-terminus of the NMDA receptor subunit NR2B regulates surface expression. *Neuropharmacology* 45: 729-737, 2003.

Legendre P, Rosenmund C, and Westbrook GL. Inactivation of NMDA channels in cultured hippocampal neurons by intracellular calcium. *Journal of Neuroscience* 13: 674-684, 1993.

Lester RA and Jahr CE. NMDA channel behavior depends on agonist affinity. *Journal of Neuroscience* 12: 635-643, 1992.

Li B, Chen N, Luo T, Otsu Y, Murphy TH, and Raymond LA. Differential regulation of synaptic and extra-synaptic NMDA receptors. *Nature Neuroscience* 5: 833-834, 2002.

Li JH, Wang YH, Wolfe BB, Krueger KE, Corsi L, Stocca G, and Vicini S. Developmental changes in localization of NMDA receptor subunits in primary cultures of cortical neurons. *Eur J Neurosci* 10: 1704-1715, 1998.

Lin Y, Skeberdis VA, Francesconi A, Bennett MV, and Zukin RS. Postsynaptic density protein-95 regulates NMDA channel gating and surface expression. *Journal of Neuroscience* 24: 10138-10148, 2004.

Liu L, Wong TP, Pozza MF, Lingenhoehl K, Wang Y, Sheng M, Auberson YP, and Wang YT. Role of NMDA receptor subtypes in governing the direction of hippocampal synaptic plasticity. *Science* 304: 1021-1024, 2004.

Liu Y, Jurman ME, and Yellen G. Dynamic rearrangement of the outer mouth of a K^+ channel during gating. *Neuron* 16: 859-867, 1996.

Low CM, Lyuboslavsky P, French A, Le P, Wyatte K, Thiel WH, Marchan EM, Igarashi K, Kashiwagi K, Gernert K, Williams K, Traynelis SF, and Zheng F. Molecular determinants of proton-sensitive N-methyl-D-aspartate receptor gating. *Molecular Pharmacology* 63: 1212-1222, 2003.

Luo J, Wang Y, Yasuda RP, Dunah AW, and Wolfe BB. The majority of N-methyl-D-aspartate receptor complexes in adult rat cerebral cortex contain at least three different subunits (NR1/NR2A/NR2B). *Mol Pharmacol* 51: 79-86, 1997.

Massey PV, Johnson BE, Moult PR, Auberson YP, Brown MW, Molnar E, Collingridge GL, and Bashir ZI. Differential roles of NR2A and NR2B-containing NMDA receptors in cortical long-term potentiation and long-term depression. *Journal of Neuroscience* 24: 7821-7828, 2004.

Masuko T, Kashiwagi K, Kuno T, Nguyen ND, Pahk AJ, Fukuchi J, Igarashi K, and Williams K. A regulatory domain (R1-R2) in the amino terminus of the N-methyl-D-aspartate receptor: effects of spermine, protons, and ifenprodil, and structural similarity to bacterial leucine/isoleucine/valine binding protein. *Molecular Pharmacology* 55: 957-969, 1999.

Mayer ML and Armstrong N. Structure and function of glutamate receptor ion channels. *Annual Review of Physiology* 66: 161-181, 2004.

Mayer ML, Vyklicky L, Jr., and Clements J. Regulation of NMDA receptor desensitization in mouse hippocampal neurons by glycine. *Nature* 338: 425-427, 1989.

McBain CJ and Mayer ML. N-methyl-D-aspartic acid receptor structure and function. *Physiological Reviews* 74: 723-760, 1994.

McIlhinney RA, Le Bourdelles B, Molnar E, Tricaud N, Streit P, and Whiting PJ. Assembly intracellular targeting and cell surface expression of the human N-methyl-D-aspartate receptor subunits NR1a and NR2A in transfected cells. *Neuropharmacology* 37: 1355-1367, 1998.

Meddows E, Le Bourdelles B, Grimwood S, Wafford K, Sandhu S, Whiting P, and McIlhinney RA. Identification of molecular determinants that are important in the assembly of N-methyl-D-aspartate receptors. *Journal of Biological Chemistry* 276: 18795-18803, 2001.

Mohrmann R, Hatt H, and Gottmann K. Developmental regulation of subunit composition of extrasynaptic NMDA receptors in neocortical neurones. *Neuroreport* 11: 1203-1208, 2000.

Mohrmann R, Kohr G, Hatt H, Sprengel R, and Gottmann K. Deletion of the C-terminal domain of the NR2B subunit alters channel properties and synaptic targeting of N-methyl-D-aspartate receptors in nascent neocortical synapses. *J Neurosci Res* 68: 265-275, 2002.

Monyer H, Burnashev N, Laurie DJ, Sakmann B, and Seeburg PH. Developmental and regional expression in the rat brain and functional properties of four NMDA receptors. *Neuron* 12: 529-540, 1994.

Mott DD, Doherty JJ, Zhang S, Washburn MS, Fendley MJ, Lyuboslavsky P, Traynelis SF, and Dingledine R. Phenylethanolamines inhibit NMDA receptors by enhancing proton inhibition. *Nature Neuroscience* 1: 659-667, 1998.

Mu Y, Otsuka T, Horton AC, Scott DB, and Ehlers MD. Activity-dependent mRNA splicing controls ER export and synaptic delivery of NMDA receptors. *Neuron* 40: 581-594, 2003.

Nong Y, Huang YQ, and Salter MW. NMDA receptors are movin' in. *Current Opinion in Neurobiology* 14: 353-361, 2004.

Okabe S, Miwa A, and Okado H. Alternative splicing of the C-terminal domain regulates cell surface expression of the NMDA receptor NR1 subunit. *Journal of Neuroscience* 19: 7781-7792, 1999.

Paoletti P, Ascher P, and Neyton J. High-affinity zinc inhibition of NMDA NR1-NR2A receptors. *Journal of Neuroscience* 17: 5711-5725, 1997.

Paoletti P, Perin-Dureau F, Fayyazuddin A, Le Goff A, Callebaut I, and Neyton J. Molecular organization of a zinc binding n-terminal modulatory domain in a NMDA receptor subunit. *Neuron* 28: 911-925, 2000.

Perez-Otano I and Ehlers MD. Learning from NMDA receptor trafficking: clues to the development and maturation of glutamatergic synapses. *NeuroSignals* 13: 175-189, 2004.

Perin-Dureau F, Rachline J, Neyton J, and Paoletti P. Mapping the binding site of the neuroprotectant ifenprodil on NMDA receptors. *Journal of Neuroscience* 22: 5955-5965, 2002.

Pickard L, Noel J, Henley JM, Collingridge GL, and Molnar E. Developmental changes in synaptic AMPA and NMDA receptor distribution and AMPA receptor subunit composition in living hippocampal neurons. *J Neurosci* 20: 7922-7931, 2000.

Pollard H, Khrestchatisky M, Moreau J, and Ben Ari Y. Transient expression of the NR2C subunit of the NMDA receptor in developing rat brain. *Neuroreport* 4: 411-414, 1993.

Qian A and Johnson JW. Channel gating of NMDA receptors. *Physiology & Behavior* 77: 577-582, 2002.

Racz B, Blanpied TA, Ehlers MD, and Weinberg RJ. Lateral organization of endocytic machinery in dendritic spines. *Nature Neuroscience* 7: 917-918, 2004.

Regalado MP, Villarroel A, and Lerma J. Intersubunit cooperativity in the NMDA receptor. *Neuron* 32: 1085-1096, 2001.

Roche KW, Standley S, McCallum J, Dune Ly C, Ehlers MD, and Wenthold RJ. Molecular determinants of NMDA receptor internalization. *Nature Neuroscience* 4: 794-802, 2001.

Rosenmund C, Feltz A, and Westbrook GL. Synaptic NMDA receptor channels have a low open probability. *J Neurosci* 15: 2788-2795, 1995.

Sans N, Petralia RS, Wang YX, Blahos J, 2nd, Hell JW, and Wenthold RJ. A developmental change in NMDA receptor-associated proteins at hippocampal synapses. *J Neurosci* 20: 1260-1271, 2000.

Sans N, Prybylowski K, Petralia RS, Chang K, Wang YX, Racca C, Vicini S, and Wenthold RJ. NMDA receptor trafficking through an interaction between PDZ proteins and the exocyst complex. *Nature Cell Biology* 5: 520-530, 2003.

Scannevin RH and Huganir RL. Postsynaptic organization and regulation of excitatory synapses. *Nat Rev Neurosci* 1: 133-141, 2000.

Schorge S and Colquhoun D. Studies of NMDA receptor function and stoichiometry with truncated and tandem subunits. *Journal of Neuroscience* 23: 1151-1158, 2003.

Scott DB, Blanpied TA, and Ehlers MD. Coordinated PKA and PKC phosphorylation suppresses RXR-mediated ER retention and regulates the surface delivery of NMDA receptors. *Neuropharmacology* 45: 755-767, 2003.

Scott DB, Michailidis I, Mu Y, Logothetis D, and Ehlers MD. Endocytosis and degradative sorting of NMDA receptors by conserved membrane-proximal signals. *Journal of Neuroscience* 24: 7096-7109, 2004.

Setou M, Nakagawa T, Seog DH, and Hirokawa N. Kinesin superfamily motor protein KIF17 and mLin-10 in NMDA receptor-containing vesicle transport. *Science* 288: 1796-1802, 2000.

Sheng M, Cummings J, Roldan LA, Jan YN, and Jan LY. Changing subunit composition of heteromeric NMDA receptors during development of rat cortex. *Nature* 368: 144-147, 1994.

Sobolevsky AI. Two-component blocking kinetics of open NMDA channels by organic cations. *Biochimica et Biophysica Acta* 1416: 69-91, 1999.

Sobolevsky AI, Beck C, and Wollmuth LP. Molecular rearrangements of the extracellular vestibule in NMDAR channels during gating. *Neuron* 33: 75-85, 2002.

Sobolevsky AI, Koshelev SG, and Khodorov BI. Probing of NMDA channels with fast blockers. *Journal of Neuroscience* 19: 10611-10626, 1999.

Standley S, Roche KW, McCallum J, Sans N, and Wenthold RJ. PDZ domain suppression of an ER retention signal in NMDA receptor NR1 splice variants. *Neuron* 28: 887-898, 2000.

Steigerwald F, Schulz TW, Schenker LT, Kennedy MB, Seeburg PH, and Kohr G. C-Terminal truncation of NR2A subunits impairs synaptic but not extrasynaptic localization of NMDA receptors. *J Neurosci* 20: 4573-4581, 2000.

Stocca G and Vicini S. Increased contribution of NR2A subunit to synaptic NMDA receptors in developing rat cortical neurons. *J Physiol* 507 (Pt 1): 13-24, 1998.

Sun Y, Olson R, Horning M, Armstrong N, Mayer M, and Gouaux E. Mechanism of glutamate receptor desensitization. *Nature* 417: 245-253, 2002.

Tong G and Jahr CE. Regulation of glycine-insensitive desensitization of the NMDA receptor in outside-out patches. *Journal of Neurophysiology* 72: 754-761, 1994.

Tovar KR, Sprouffske K, and Westbrook GL. Fast NMDA receptor-mediated synaptic currents in neurons from mice lacking the epsilon2 (NR2B) subunit. *J Neurophysiol* 83: 616-620, 2000.

Tovar KR and Westbrook GL. The incorporation of NMDA receptors with a distinct subunit composition at nascent hippocampal synapses in vitro. *J Neurosci* 19: 4180-4188, 1999.

Tovar KR and Westbrook GL. Mobile NMDA receptors at hippocampal synapses. *Neuron* 34: 255-264, 2002.

Townsend M, Yoshii A, Mishina M, and Constantine-Paton M. Developmental loss of miniature N-methyl-D-aspartate receptor currents in NR2A knockout mice. *Proc Natl Acad Sci U S A* 100: 1340-1345, 2003.

Traynelis SF, Hartley M, and Heinemann SF. Control of proton sensitivity of the NMDA receptor by RNA splicing and polyamines. *Science* 268: 873-876, 1995.

Vicini S, Wang JF, Li JH, Zhu WJ, Wang YH, Luo JH, Wolfe BB, and Grayson DR. Functional and pharmacological differences between recombinant N-methyl-D-aspartate receptors. *J Neurophysiol* 79: 555-566, 1998.

Villarroel A, Regalado MP, and Lerma J. Glycine-independent NMDA receptor desensitization: localization of structural determinants. *Neuron* 20: 329-339, 1998.

Vissel B, Krupp JJ, Heinemann SF, and Westbrook GL. A use-dependent tyrosine dephosphorylation of NMDA receptors is independent of ion flux. *Nature Neuroscience* 4: 587-596, 2001.

Wenthold RJ, Prybylowski K, Standley S, Sans N, and Petralia RS. Trafficking of NMDA receptors. *Annual Review of Pharmacology & Toxicology* 43: 335-358, 2003.

Wilson GG and Karlin A. The location of the gate in the acetylcholine receptor channel. *Neuron* 20: 1269-1281, 1998.

Wollmuth LP and Sobolevsky AI. Structure and gating of the glutamate receptor ion channel. *Trends in Neurosciences* 27: 321-328, 2004.

Wyszynski M, Lin J, Rao A, Nigh E, Beggs AH, Craig AM, and Sheng M. Competitive binding of alpha-actinin and calmodulin to the NMDA receptor. *Nature* 385: 439-442, 1997.

Yang N and Horn R. Evidence for voltage-dependent S4 movement in sodium channels. *Neuron* 15: 213-218, 1995.

Zhang S, Ehlers MD, Bernhardt JP, Su CT, and Huganir RL. Calmodulin mediates calcium-dependent inactivation of N-methyl-D-aspartate receptors. *Neuron* 21: 443-453, 1998.

Zheng F, Erreger K, Low CM, Banke T, Lee CJ, Conn PJ, and Traynelis SF. Allosteric interaction between the amino terminal domain and the ligand binding domain of NR2A. *Nature Neuroscience* 4: 894-901, 2001.

Zhong J, Russell SL, Pritchett DB, Molinoff PB, and Williams K. Expression of mRNAs encoding subunits of the N-methyl-D-aspartate receptor in cultured cortical neurons. *Mol Pharmacol* 45: 846-853, 1994.